N 70 17511

NASA CR 107876

FINAL REPORT
LIGHT-WEIGHT WOLF TRAP STUDY

5 Nov 1969

BALL BROTHERS
RESEARCH CORPORATION
LABORATORIES IN BOULDER, COLORADO AND MUNCIE, INDIANA

BALL BROTHERS RESEARCH CORPORATION

BOULDER, COLORADO

FINAL REPORT
LIGHT-WEIGHT WOLF TRAP
STUDY

F69-05 5 Nov 1969

Prepared for

University of Rochester
Rochester, New York

APPROVED

D E Buckendahl

D. E. Buckendahl
Project Manager

D B Hicks

D. B. Hicks
Dept. Manager,
Advanced Programs

FOREWORD

This report has been prepared for the University of Rochester under agreement NsG-209 AG-1 entitled "Wolf Trap Microbe Detection Device." It constitutes the final report on Modifications 9 and 10, for a Lightweight Wolf Trap study; and on Modification 11, for an infrared detector study and start on mechanical modeling.

BBRC personnel who participated in both performance of the study and in preparation of this report include: F. G. Brown, infrared detector; D. E. Buckendahl, system design; V. H. Henthorn, mechanical system design; J. D. Pace, light-scatter optics; and A. J. Ray, electronics.

SUMMARY

In late 1968, BBRC initiated the preliminary design of a small, light-weight Wolf Trap Life Detection Device. The design is intended for use on the Viking lander vehicle being considered for a 1973 Mars landing.

Since the pH sensor on the Wolf Trap models designed earlier were relatively insensitive, a feasibility study was performed on detection of carbon dioxide gas above a soil sample, which would be supplied with nutrients and exposed to the Mars atmosphere. At the termination of the study, an infrared detector had been designed which has a calculated minimum carbon dioxide detection level of 10^{-11} gram moles.

Three different light-scatter cell configurations were constructed and tested. The light scatter cell is used to measure the particles present in a liquid solution, thus providing another means for detecting the presence and growth of live organisms. A breadboard model of the third configuration tested showed good detection sensitivity and a subsequent test model built and tested briefly before the program ended gave good results, although some further refinement of the system would be necessary.

The necessary electronics for the light scatter cell were also designed and tested. The final configuration was a differential system using a reference compensated for stray light and temperature. The testing performed on the differential system indicated that it would be a significant improvement over the system used in the earlier Wolf Trap model; however, comprehensive testing of the system would be needed to fully verify its performance.

In addition to the work on components, a preliminary flight-configuration system design was evolved. This design is a carousel type capable of testing nine samples and would weigh approximately 10 pounds, including electronics.

CONTENTS

ILLUSTRATIONS

Section 1
INTRODUCTION

Since 1963 Ball Brothers Research Corporation has been involved in development of the Wolf Trap Life Detection Device. A flight-configured engineering model was built, tested, and delivered in 1967. That model combined two measurements: light scattering from particles in solution and pH monitoring in the solution. The configuration was intended for the large-class Mars soft lander being considered at that time. Subsequent studies were performed to develop concepts of smaller mechanisms and optical systems.

Then, in late 1968, all effort was directed to the preliminary design of an instrument for the 1973 Viking lander which was under study. However, testing of the pH system had shown the method was too insensitive an indicator of activity to be used with the highly sensitive light scattering measurement. Since, historically, the Wolf Trap concept has required the direct measurement of both organism growth and of solution activity, a feasibility study was performed on detection of carbon dioxide gas above a soil culture. The philosophy guiding the total instrument development concept has been that the device must serve as a backup to the integrated biology experiment currently being developed under direction of the NASA-Ames Research Center. However, a backup is not a backup if it is more complex than the primary instrument. Therefore, principal design goals have been simplicity of design with minimal dependence on components requiring additional development, and reduction in end-item cost by modular design that permits repetitive machining operations.

A detailed discussion of the results and the recommendations for each of the major areas of the feasibility study is presented in separate, detailed sections of this report. Thus, the light scatter cell, the infrared detector, and the electronics, are covered in Sections 2, 3, and 4, respectively. Section 5 presents a discussion of the system design philosophy and describes the flight-configuration concept developed as a result of this study.

Section 2
LIGHT SCATTER CELLS

The light scatter cells illuminate a liquid solution and detect light scattered by particles in the solution. The intensity of the scattered light approaches zero if the liquid is distilled, filtered and degassed water. When biological organisms or other small particles are present, the light scattered is a function of the number of scattering particles in the liquid. By separating and detecting the scattered light from the input light, it is possible to determine the increase in number of particles in the liquid.

2.1 OPTICAL SYSTEMS

Three light scatter cell configurations were constructed and tested. The cells differ principally in the method of collecting scattered light. In all three configurations, a spherical mirror forms one side of the cell and is illuminated from a light source located at the radius of curvature of the mirror. The emergent light first passes through the liquid; it is then reflected back through the liquid and focused onto the source. The scattered light is collected and converted into an electrical signal by a photodetector.

The first configuration, shown in Fig. 2-1, provides illumination through a single fiber optic which also collects the non-scattered light reflected from the mirror. The scattered light (dashed line) is multiply reflected back to the detector. Light losses from reflections reduced the sensitivity of a practical system to detection of about 10^7 E. Coli. per milliliter.

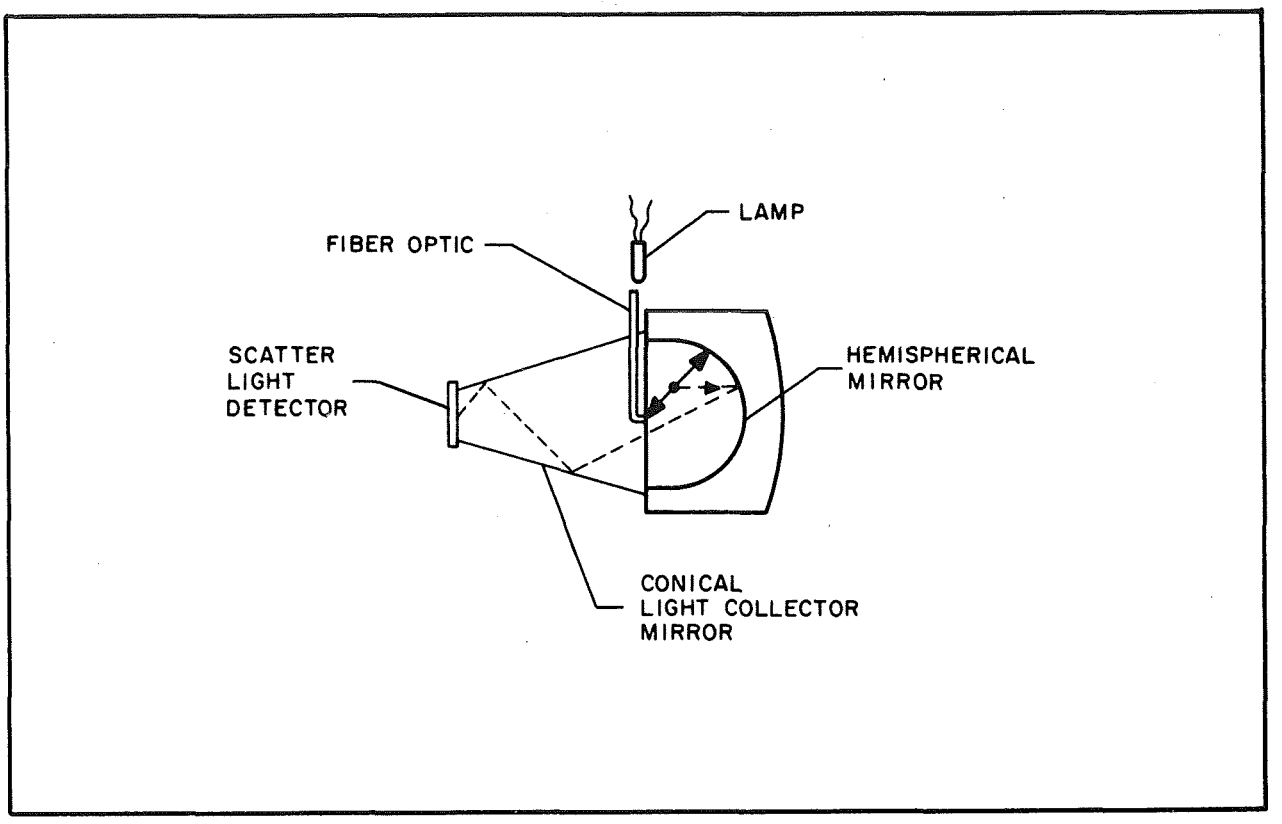

Fig. 2-1 Conical-Mirror Collector

The second cell, shown in Fig. 2-2, admits light through a pinhole aperture in the collector mirror, which images the scattered light onto the detector. The mirror is limited in physical size so that only about a 10-degree cone of scattered light can be collected. The system is limited to detection of about 2×10^5 microorganisms per milliliter.

The third system is shown in Fig. 2-3. Losses in the other configurations suggested that the fewer the optical components and light reflections, the better the sensitivity would be. In this cell, the light from the lamp source is piped down a single fiber optic, through a silicon photodetector and transparent face plate, and emerges at the radius of curvature of the mirror. The scattered

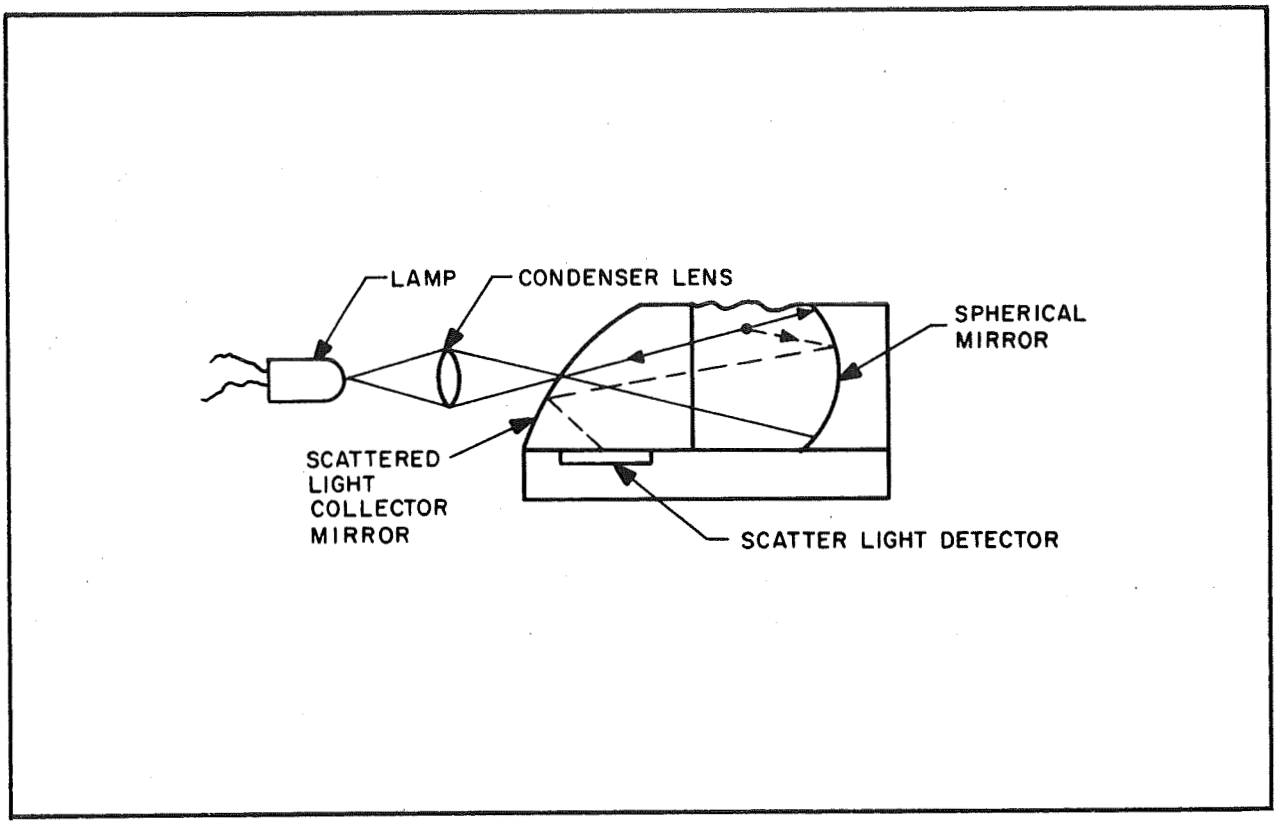

Fig. 2-2 Off-Axis Mirror Collector

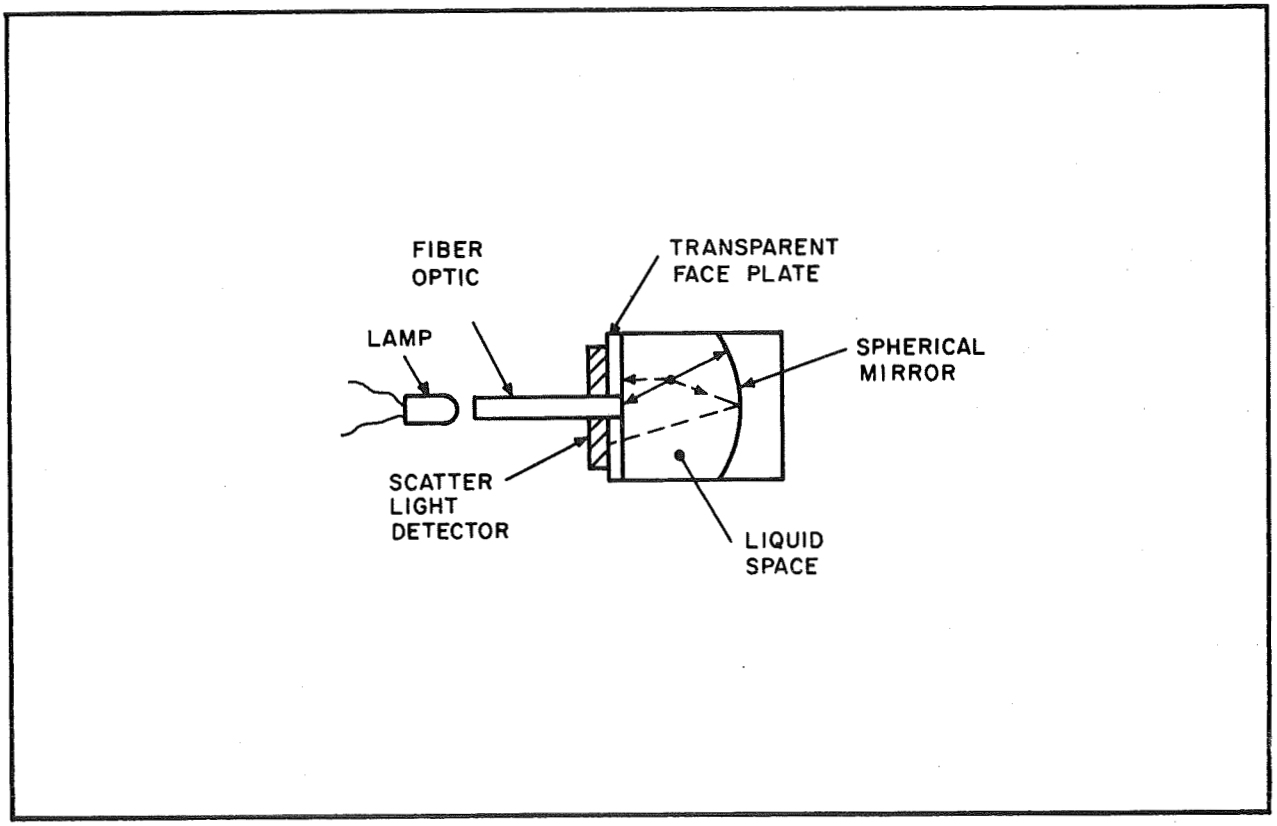

Fig. 2-3 Plane-Detector Collector

light is intercepted by the detector, either after reflection from the mirror or directly from the particle after the illuminating ray has reflected from the mirror.

A breadboard model of this system was tested for response to E. Coli. in media at 37°C. The media consisted of bacto-tryptone, sodium chloride, and thiamine hydrochloride in quantities optimum for the organism. Generation time is about 25 minutes. Two successive and identical tests yielded the results shown in Fig. 2-4. The curve's slope change at 70 minutes has been observed in previous testing with the engineering model of the Wolf Trap. However, the step at 60 minutes had not been detected previously because it occurs at low populations not tested before. System stability was continuously monitored during the test and showed nothing that could produce changes greater than 0.2 arbitrary light-scatter units.

It must be noted that only a terminal plate count was made for the test. The scale for population estimate in Fig. 2-4 is based solely on the estimated generation time. Inoculum was a log-phase culture and was estimated to be 500 organisms per milliliter, in agreement with the 25-minute generation time and the terminal count.

The breadboard model, although showing good detection sensitivity, has some problems which must be resolved for a flight application. These are discussed in subsection 2.2 below.

2.2 OPTICAL IMPROVEMENTS

The problems encountered in the breadboard model were

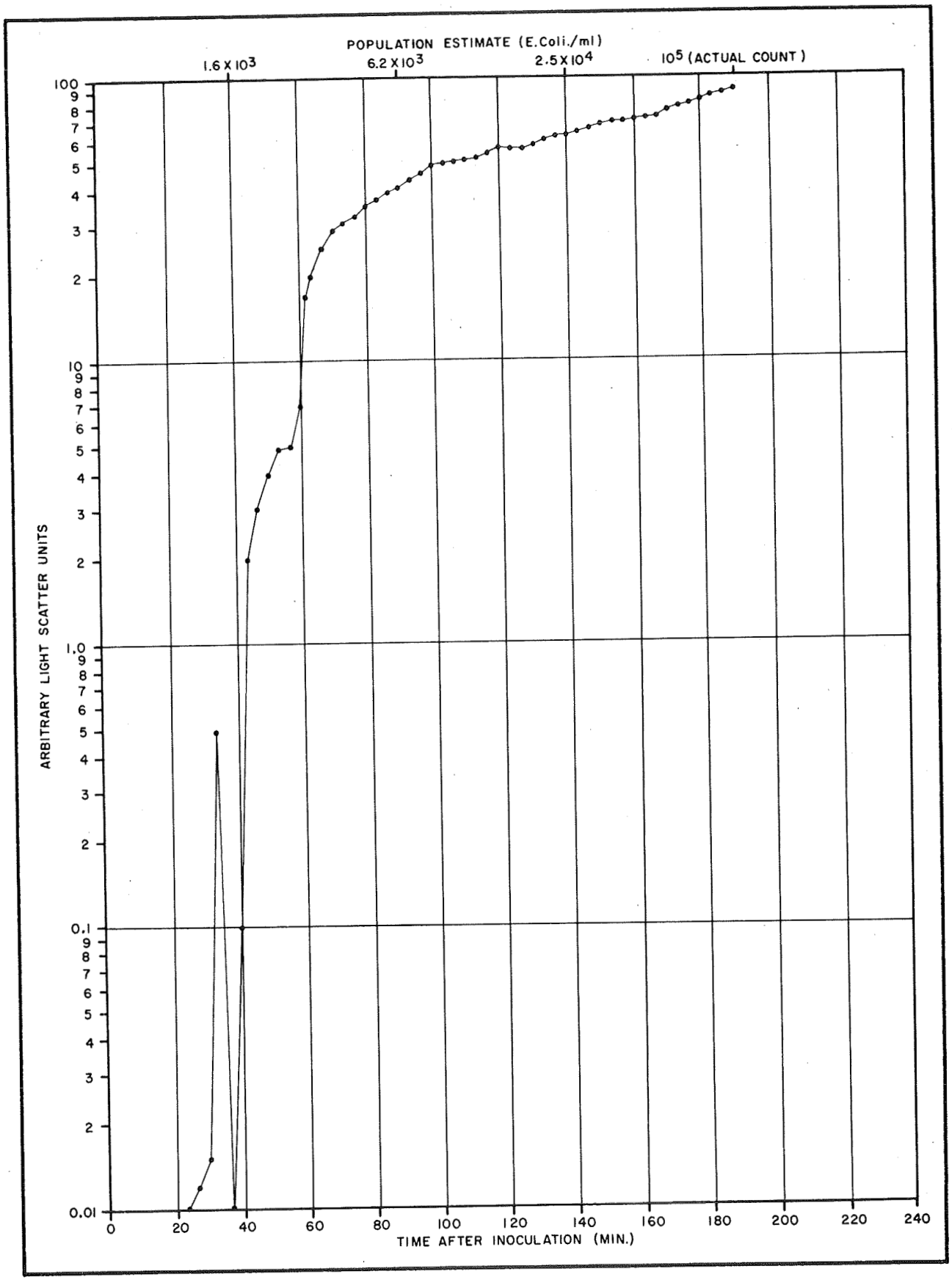

Fig. 2-4 E. Coli. Growth Test

1) high output current from stray light

2) temperature change instability of output

3) detector noise masking low signals

The high current caused by stray light is undesirable because small changes in illumination intensity produce detector signal changes which are much larger than the light scattering signals. Temperature instability is caused by differences in response between the light scatter detector and the detector used as a reference to compare light source intensity. In the breadboard model tested, the reference detector received light directly from the source, while the scatter detector light was modified by the absorption bands of the water and the media. The detector-generated random noise totally masks the scattered light signal at low current levels. Fig. 2-4 shows this effect between 20 and 40 minutes.

To provide a test bed for improvements, a versatile test unit was fabricated and is shown in Fig. 2-5. All metal in contact with the media is titanium alloy, 6AL-4V. The spherical glass mirror is chromium-plated and overcoated with silicon monoxide, which was found necessary after galvanic cell corrosion had marred two earlier mirrors. The optic carrier presses the transparent face plate against the cell body O-ring seal and provides attachment points for the light source (not shown). Cell capacity is 5 milliliters total, including plumbing connections for the trial peristaltic pump. Actual liquid volume within the optical detector is 2 milliliters.

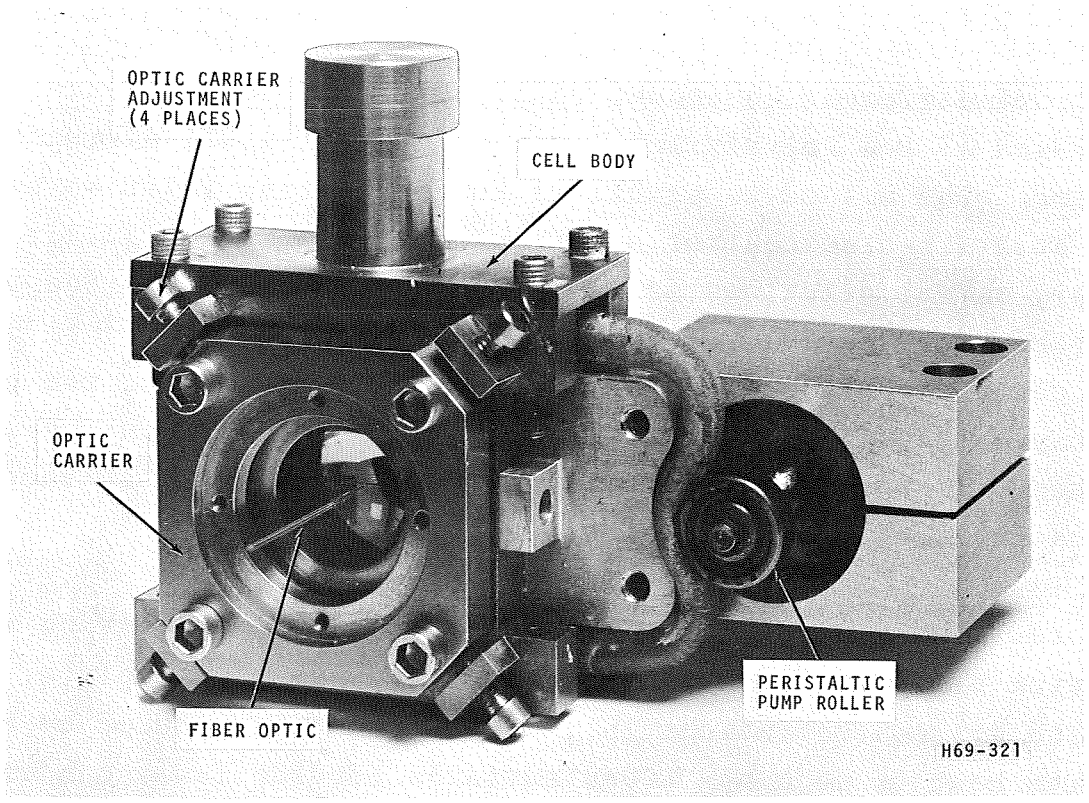

(Front)

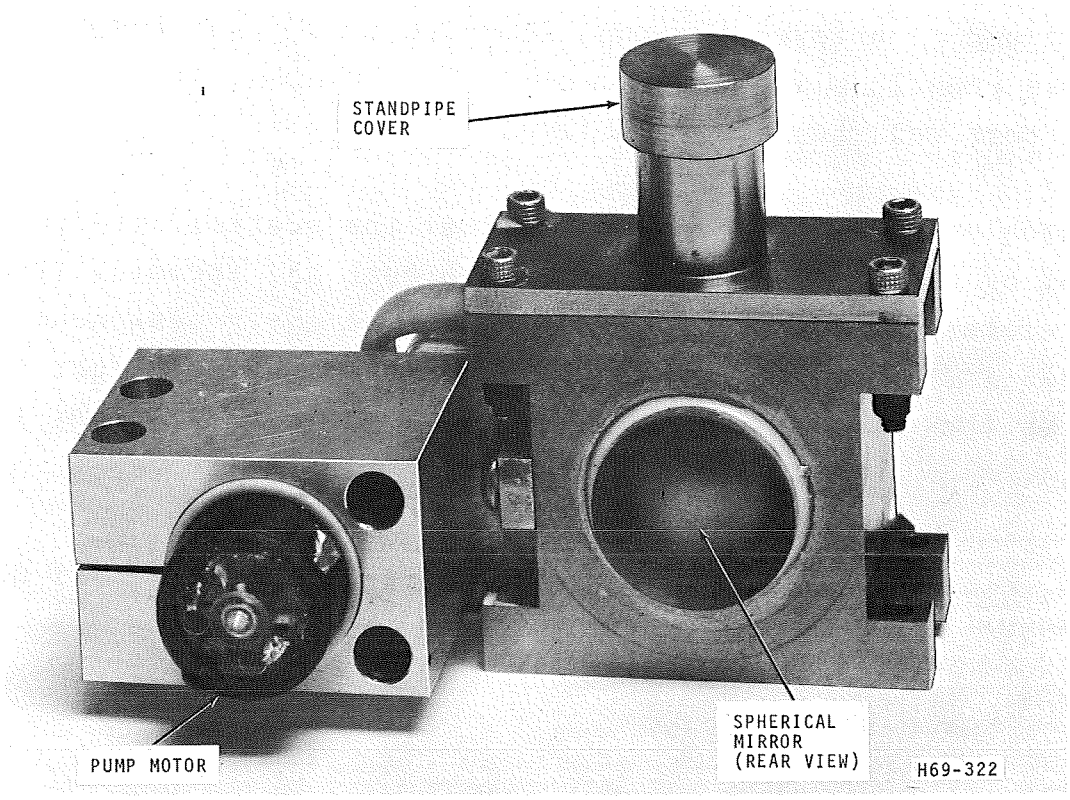

(Back)

Fig. 2-5 Cell Components Test Model

Testing of different component configurations was done using a water dispersion of Dow Polystyrene latex spheres of 1.011-microns diameter. The method is practical for evaluating relative performance at a fixed concentration of 10^6 particles per milliliter. However, serial dilutions of the suspension did not provide an acceptable calibration technique. The spheres readily form clumps which can be separated only by severe agitation. Also, the particles have a great tendency to cling to electrically non-conductive surfaces. This effect is attributed to electrostatic attraction, but has not been conclusively proven.

Undoubtedly, the worst operational problem found in testing is the formation of minute gas bubbles on the mirror and faceplate. Adsorbed gas concentrations in the water must be reduced by boiling with heat or vacuum. Clean surfaces provide fewer condensing nuclei, but superior operational cleanliness is difficult to achieve. The peristaltic pump, if operated so that water left the cell bottom and re-entered the top, introduced no significant gas bubbles. Reverse pump flow flooded the cell with bubbles, even with the top inlet port well below liquid level.

The problem of reducing stray light at the scatter detector can be solved by isolating the detector from both the incoming light and the refocused image at the faceplate. The early test model used a 0.028-inch diameter single glass fiber to conduct light into the cell as shown in Fig. 2-6. A previous study[1] showed that light

---

[1] BBRC, Final Report, Wolf Trap Miniaturization Study, F69-01, 29 August 1969, p. 3-17.

refocused back onto the fiber is spread by about 50 percent in diameter. This unwanted light falls on the detector and increases the background signal. Also, minute fractures at the end of the fiber, formed as a natural consequence of fabrication of glass parts, allow some incoming light to bleed into the faceplate and onto the detector.

The method of detector isolation tried was use of a fiber optic faceplate as shown in Fig. 2-7. The faceplate consists of glass fibers of micron-range diameter, coated with absorptive material and fused together, with the fiber direction normal to the faceplate surface. Light transmission between fibers is minimized by the coating absorption. The input light is focused on the faceplate and emerges on the other side at a maximum angle controlled by the fiber's numerical aperture. Reflected and spread light is conducted past the detector's sensitive area, while scattered light is directed onto that area. Some improvement was achieved in the scatter current/background current ratio over the 5 to 1 ratio obtained in the system previously used.[2] The method also provides a smooth, continuous faceplate surface which reduces gas bubbles condensing at crevice nuclei.

The problem of scatter-detector-generated noise is discussed in subsection 4.2. The solution is modulation of the light at a frequency above 25 Hz to permit use of selectively tuned amplifiers that will not be affected by noise frequencies outside

---

[2] Ibid., p. 3-20.

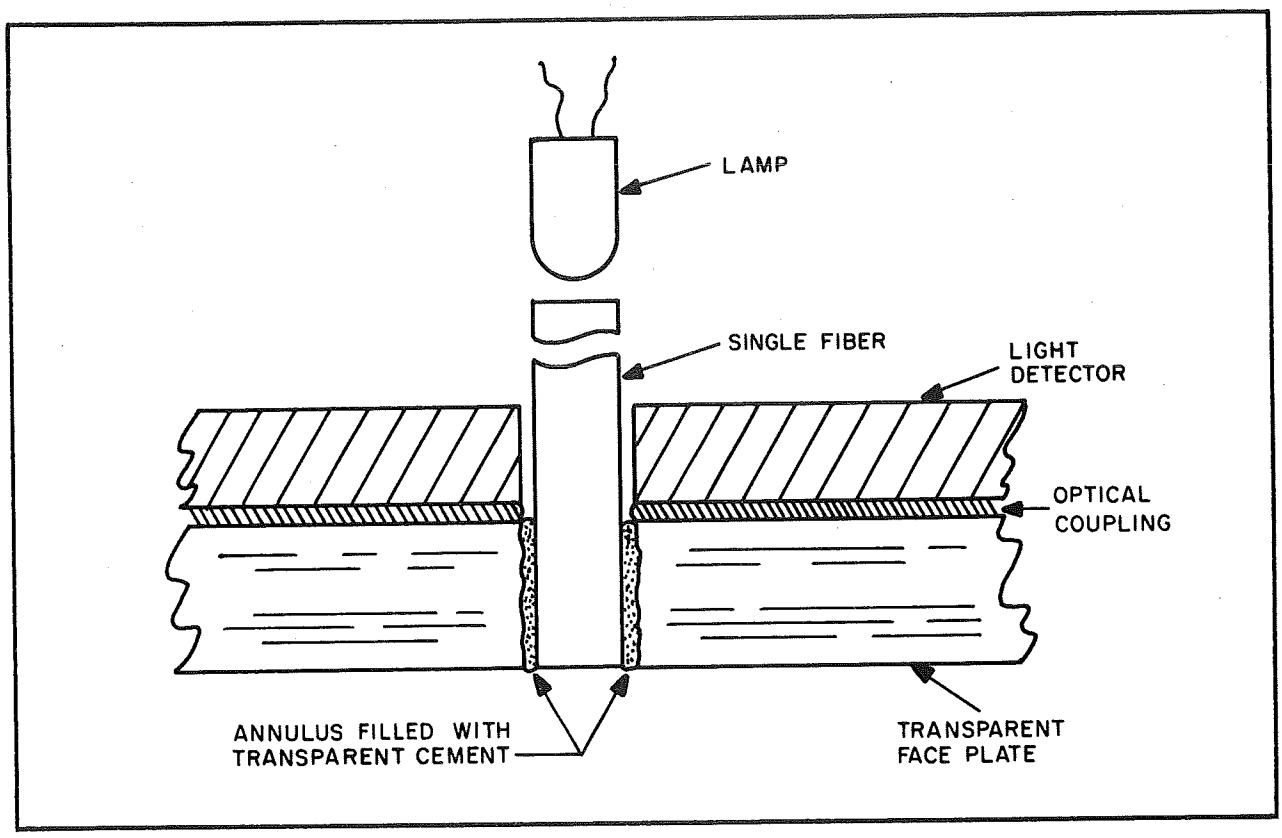

Fig. 2-6 Single-Fiber Light Pipe

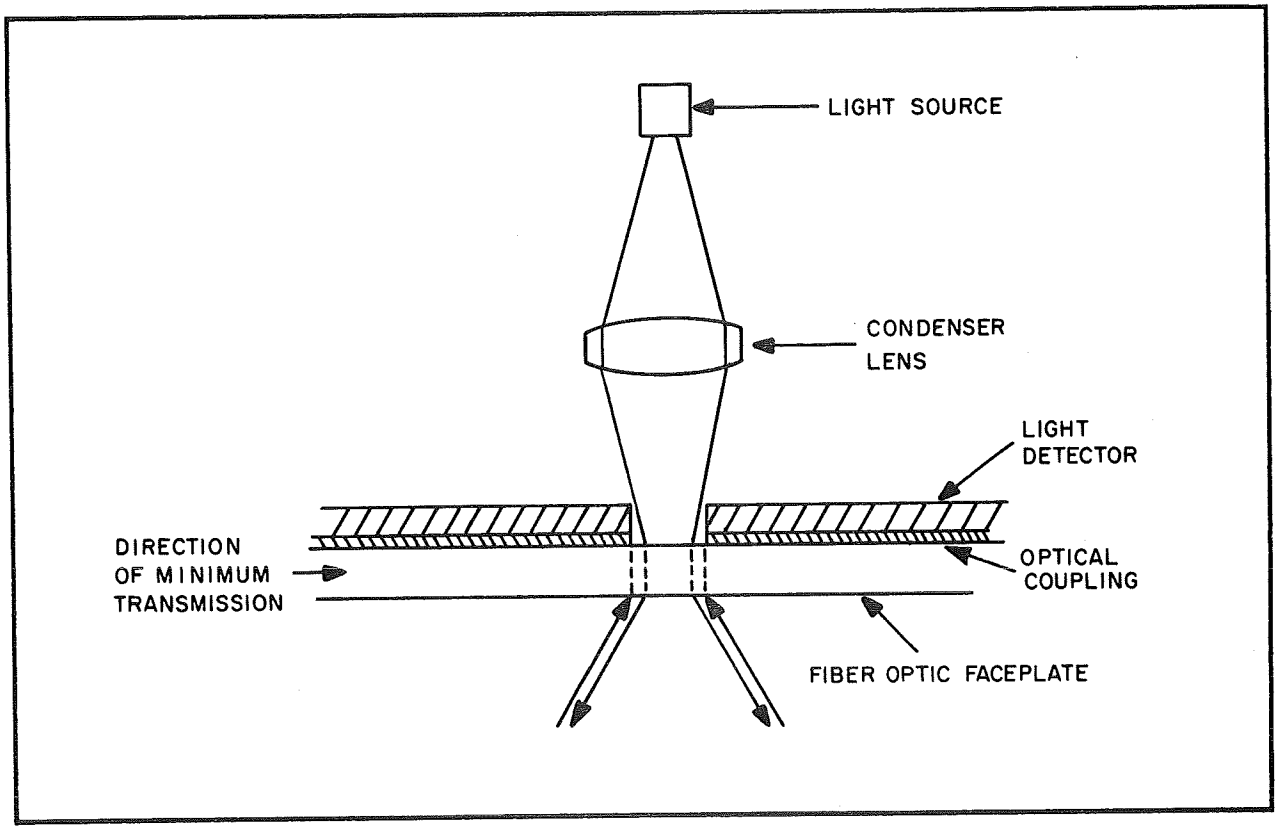

Fig. 2-7 Fiber Optic Face Plate

their band pass. The light detector characteristics limit the maximum frequency to about 800 Hz, well above the calculated 25 Hz. Modulation of incandescent lamps by the power input is not possible because of the filament's thermal inertia. Certainly a rotating shutter could be used in front of a constantly burning lamp, but the method is mechanically complex. An alternate approach is pulsing a light-emitting semiconductor.

A variety of light-emitting semiconductors are available for use as a pulsed light source. The principal advantages for use with a light scatter detector are small source size, high reliability and fast response at high pulse rates. The devices have a narrow-wavelength emission band which can be centered from the visible to near infrared. Some feeling for sterilization temperature resistance was obtained when a commercially available unit was passively baked. A Monsanto MV-10B gallium arsenside phosphide (GaAsP) diode with an integral epoxy lens emits at 0.67 micron. After dry heat sterilization at 155°C for a 20-hour and a 44-hour period, the light output dropped 7.2 percent from lens darkening. Other devices have glass lenses which should be satisfactory.

The problem of temperature sensitivity of light detectors is the most severe problem of the three. Any light detector output will vary with temperature at fixed illumination. Ideally, a detector system has nearly constant illumination with provision for monitoring and correcting coarse changes, and has an output independent of temperature and fine illumination changes.

Previous detector systems used a light detector to control illumi-

nation and another detector for measuring light scattering. However, light absorption in the water altered the spectral sensitivity of the scatter detector so as to make the system response nonlinear with temperature.

A solution to the temperature problem is the use of differentially connected light detectors, as discussed in subsection 4.1. A test setup was constructed and tested to evaluate this method. The test setup is shown in Fig. 2-8. The arrangement is the same as in Fig. 2-7, except that a thin, transparent piece of glass plate is inserted in the path of the illuminating light beam. About four percent of the incident light is reflected from the beam splitter onto the monitor which is used to control the light source power. Also, about four percent of the reflected and focused light is directed onto the reference detector, which is electrically combined with the scatter detector to provide a differential output largely independent of small changes in illumination. The arrangement allows placement of all three detectors into a small assembly which has a minimum temperature gradient. This, together with the reference and scatter detectors receiving water-filtered light, produced little temperature change in output.

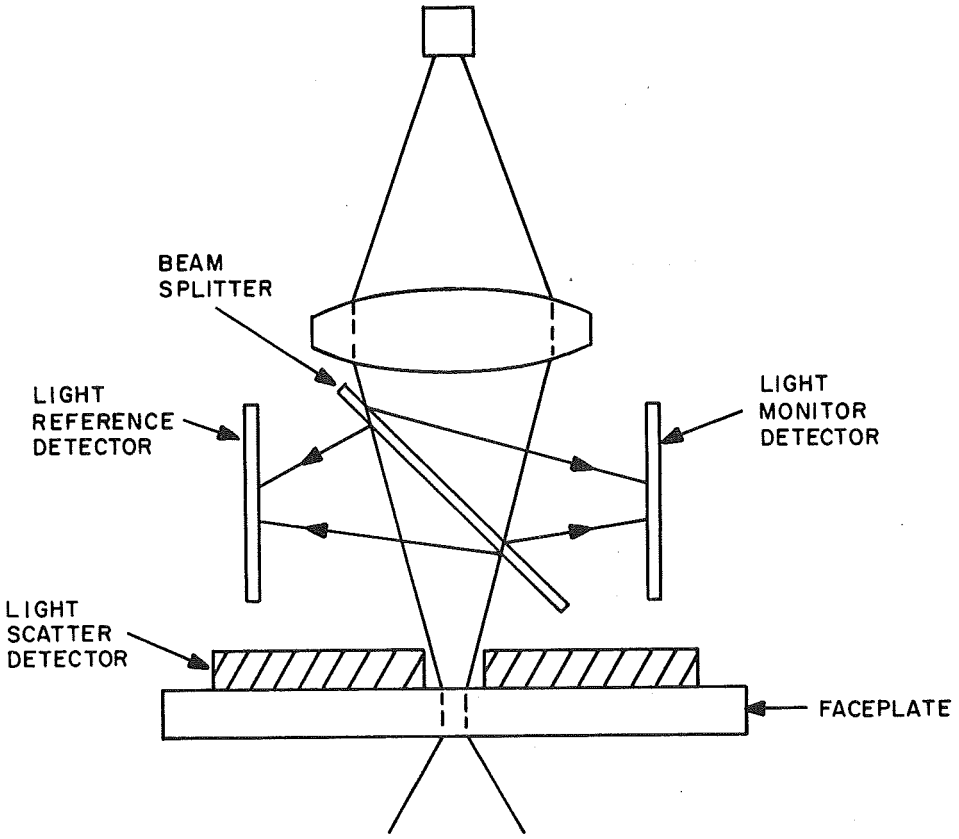

Fig. 2-8 Differential Detector and Beam Splitter

Section 3
INFRARED DETECTOR

3.1 CONCEPT DESIGN

A report from Langley Research Center, dated February 1969, shows the surface pressure of Mars is probably 9mb. Approximately 68.5 percent of the atmosphere is CO_2, with nitrogen and argon the other constituents.[1]

Assuming life exists on Mars, it might be detected by placing a soil sample in a nutrient-rich water bath open to a cell containing the normal Martian atmosphere. Detection would be accomplished by measuring changes in the absorption of infrared radiation passing through the cell due to an increase or decrease of carbon dioxide concentration within the volume. The low pressures encountered on Mars would allow the water to vaporize rapidly, with possible carryover of water droplets into optical windows, but the cell could be overpressured with nitrogen or helium to prevent the problem. An overpressure to 100 mm Hg would probably be sufficient to retard vaporization.

A review of available uncooled detectors and data on CO_2 absorption indicates that the 4.25-micron absorption band is the best for detection. Band selection requires determining the optimum center frequency and bandpass for detection at the Martian CO_2 concentration and total overpressure. A realistic infrared "spike" bandpass filter can be manufactured with a bandpass, at the 50 percent-of-maximum-transmission points, of between 1 and 1-1/2 percent of the center wavelength. The

---

[1] NASA, Viking Project, Mars Engineering Model, M73-106-0, NASA Langley Research Center, Viking Project Office, 1969.

5-percent-of-maximum-transmission points can be assumed to be approximately twice this width. Therefore, it is reasonable to assume that a filter may be obtained for use in the 4.25-micron band that is 0.08 microns wide at the 50-percent-of-maximum-transmission points, and 0.16 microns wide at the 5-percent-of-maximum-transmission points. A filter with these characteristics may be approximated by a "perfect" filter 0.10 microns wide at the maximum and zero transmission points.

Howard, et al.,[2] have shown empirical relations between the variables causing absorption change and the total band absorption. These relations were derived from previous theoretical work. The work of Burch, et al.,[3] shows the results of experimental measurements using parameters nearly equal to those required for a life detection system. Comparing results from Burch to those obtained by Howard suggests that the experimental measurements may be used as a basis for making the above determinations. Further, a paper by Andreyev and Pokrovskiy[4] substantiates this deduction by a comparison of other theoretical work to that of Burch.

---

[2]J. N. Howard, D. E. Burch, and D. Williams, "Infrared Transmissions of Synthetic Atmospheres, Part II, Absorption by Carbon Dioxide", J. Opt. Soc. Am., Vol. 46, 1956, p. 237.

[3]AFCRL, Infrared Absorption by Carbon Dioxide, Water Vapor, and Minor Atmospheric Constituents, by D. E. Burch, D. Gryvnak, E. B. Singleton, W. L. France, and D. Williams, AFCRL-62-698 Research Report, Bedford, Mass., AFCRL, Geophysics Research Directorate, 1962.

[4]S. D. Andreyev and A. E. Pokrovskiy, "The Theoretical Infrared Spectra of H_2O and CO_2 as Compared with Laboratory Measurements", Bull. Acad. Sci. U.S.S.R., Div. Atmos. and Ocean Phys., Vol. 4, 1968, pp. 671-675.

The partial pressure of CO_2 in the Martian atmosphere is

$$9\text{mb} \times 0.685 = 6.16 \text{ mb}$$

or approximately 0.0061 standard atmospheres at the Martian most-probable surface temperature of 230°K. Reduced to standard temperature, this becomes:

$$P_{ST} = \frac{273}{230} \times 0.0061 = 0.00724 \text{ std atm}$$

If a gas cell path-length of 10 cm is selected, the CO_2 concentration may be expressed as:

$$0.00724 \text{ atm} \times 10 \text{ cm} = 0.0724 \text{ atm-cm}$$

The absorption of infrared in the cell will depend on the partial pressure of the CO_2 and the total pressure, as a result of the different absorption-broadening abilities of the gases involved. Burch has suggested the broadening effects of two gases can be expressed in terms of a single variable, called the equivalent pressure, and defined by $P_E = P + 1.30p$, where P is the total pressure of a binary mixture of nitrogen and CO_2, and p is the partial pressure of the CO_2. Since the other constituents in the Martian atmosphere would be a very small percentage of the total pressure, this equation should apply in the present system. With the gas variables set as above, P_E will equal approximately 106 mm Hg.

The experimental data of Burch has been studied to determine the optimum center wavelength, and it appears to be 4.27 microns, with the 50-percent-of-maximum-transmission points at 4.23 and

4.31 microns. The data was then reduced to graphical data shown in Fig. 3-1. This graph shows $\int A(V)dV$ vs. CO_2 concentration over the range of interest. $\int A(V)dV$ may be converted to the absorption factor through division by 55, which is the bandwidth in cm^{-1}. Further conversion to percent absorption may be accomplished through multiplication by 100. From the graph, it can be seen that for every 0.01 atm-cm concentration change of CO_2, there will be an absorption change of 2.73 percent in the vicinity of 007 atm-cm concentration. This concentration change is equivalent to a CO_2 partial pressure change of 0.001 atm in a 10-cm path-length cell.

Three modes of operation for an instrument have been considered: a two-wavelength, single-beam mode; a single-wavelength, dual-beam mode with a reference cell; and a two-wavelength, dual-beam mode.

The two-wavelength, single-beam mode would detect changes in CO_2 by alternately sampling absorption in the gas sample cell at two wavelengths. One wavelength would be the CO_2 absorption wavelength, and the other must be selected in a nearby infrared "window" (3.5 to 4.15 microns). The latter would be used as a reference and must not present any change in absorption characteristics due to any possible culture-generated gases. However, the wavelengths available for window operation fall in a region where methane absorption is small but broad in spectrum. Also, nitrous oxide, a possible but unlikely gas, absorbs at the window wavelength.

The single-wavelength, dual-beam mode would detect changes in CO_2 by alternately sampling the absorption between a sample cell and a gas reference cell. The absorption wavelength, again,

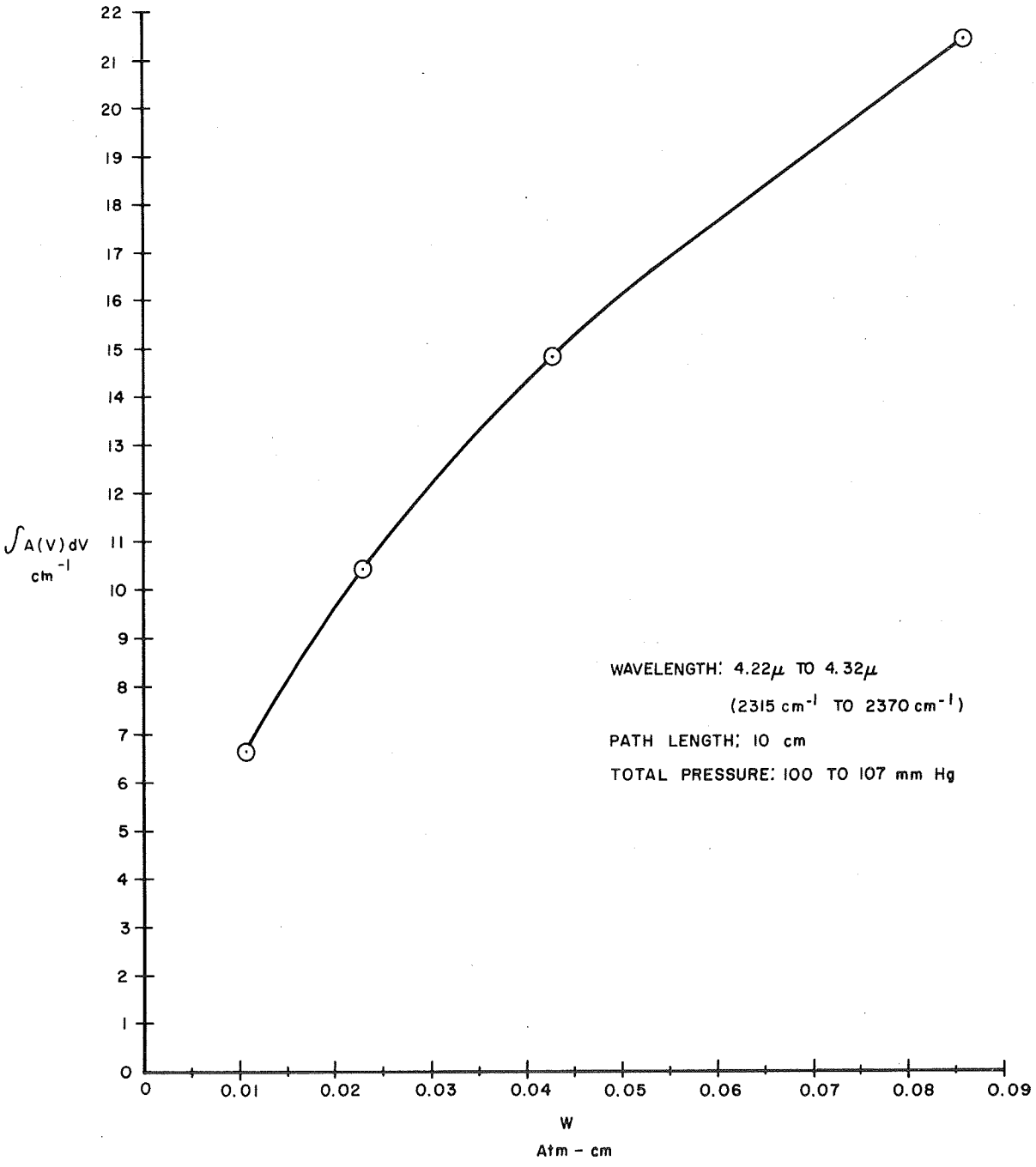

Fig. 3-1 $\int A(u)dV$ vs CO_2 Concentration

would be at 4.27 microns. This mode is used in Fig. 3-2, which shows a layout of a flight-configured system.

The two-wavelength, dual-beam mode would detect CO_2 by the same method as the single-wavelength, dual-beam mode and could also be used for detection of other gases by using the second wavelength centered on a different absorption maximum. The system design would be more complicated by the requirement of inserting alternately different filters in front of a single detector, or of using a second detector, properly filtered and located adjacent to the other detector.

Considerations of power, space and weight have led to selection of a 1000°C blackbody infrared source with a 1.5mm aperture. Planck's equation is

$$W = \frac{c_1}{\lambda^5} \left(e^{c_2/\lambda T} - 1\right)^{-1}$$

where W = the radiation emitted by a black body per unit surface area per unit wavelength interval into a hemisphere

T = the absolute temperature in degrees Kelvin

λ = wavelength of emitted radiation in cm

e = 2.718

$c_1 = 3.7402 \times 10^{-12}$ watt-cm^2

$c_2 = 1.43848$ cm-deg

The equation may be numerically or graphically integrated over the wavelength region of 4.22 to 4.32 microns. The result is a total power radiated into a hemisphere of 2.25×10^{-1} watts per

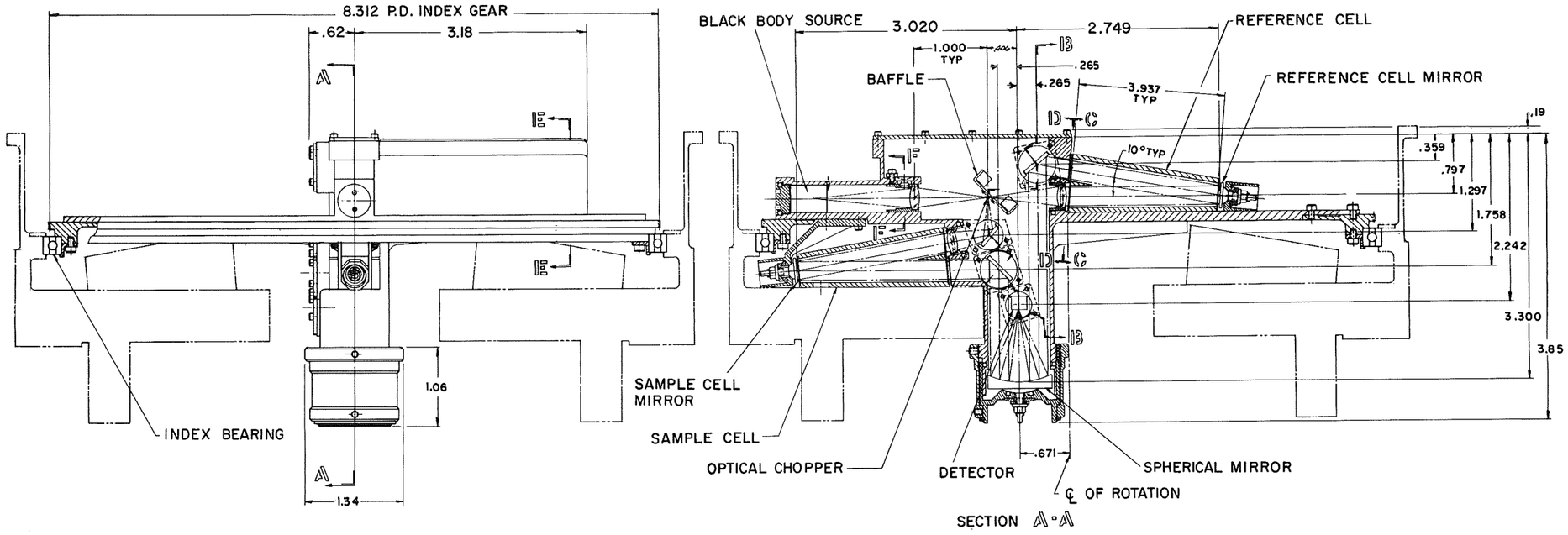

Fig. 3-2 Infrared Gas Concentration Detector

square centimeter of aperture. The total radiation from the selected blackbody is:

$$2.25 \times 10^{-1} \text{ watts/cm}^2 \times \pi\frac{(0.15)^2}{4} \text{ cm}^2 = 2.98 \times 10^{-3} \text{ watts}$$

An evaluation of available uncooled detectors usable at the wavelength of interest has indicated lead selenide to be the best choice to perform the desired operation. A report by Johnson, et al.[5], shows that maximum D* (detectivity) occurs at the desired wavelength for CO_2 concentration change detection. Also, conversation with one detector manufacturer revealed that a lead selenide detector has survived 175°C for several hours, and that the device appears capable of withstanding the extended 135°C sterilization cycles.

Referring to Fig. 3-2, it can be seen that a beam-deflecting optical chopper is required at the first image point of the source in order to pass the infrared alternately through the sample and reference cell. A tuning-fork chopper fitted with a mirror 4mm long and 2mm wide can be used to perform this operation. Size considerations and required chopping frequencies for the detector set the chopping rate at 1000 Hz.

Due to the large number of optical components in the system, it is necessary that all window materials have a high transmittance and that the mirrors have a high reflectivity. This requirement may be met by having the lenses and windows fabricated of polycrystalline magnesium fluoride. The mirrors may be a gold layer over any suitable substrate compatible with the rest of the instrument.

---

[5]T. H. Johnson, H. T. Cozine, and B. N. McLean, "Lead Selenide Detectors for Ambient Temperature Operation", Applied Optics, Vol. 4, No. 6, June 1965, pp 693-696.

The system illustrated, using cells charged with gases as mentioned, will have an optical efficiency of approximately 50 percent. However, the system must be purged of all CO_2, with the exception of the reference and sample cells. The effective f number of the first lens is f4. Therefore, the radiant power entering the optical system will be reduced from that leaving the source by a factor of approximately 8×10^{-3}. The power entering the system is:

$$3.98 \times 10^{-3} \text{ watts} \times 8 \times 10^{-3} = 3.18 \times 10^{-5} \text{ watts}$$

Considering the 50 percent efficiency of the optical system, the power at the detector will be:

$$3.18 \times 10^{-5} \text{ watts} \times 0.5 = 1.59 \times 10^{-5} \text{ watts}$$

Reference to Johnson[6] shows the D* at 4.27 microns and 10kHz of a typical lead selenide detector operating at 283°K to be approximately 1.8×10^{10} cm-$Hz^{1/2}$/watt. Consultation with manufacturers indicates that this figure is slightly high, and that D* at the same wavelength, but at 1 kHz, may be near 4×10^{9}. The frequency of 1 kHz for the latter is the same as suggested above for the instrument design. Therefore, 4×10^{9} will be assumed to be a valid figure.

A determination of percent of power absorption detectable may be derived by converting D* to another figure of merit, Noise Equivalent Power (NEP), as follows:

$$NEP = \frac{(A\ \Delta f)^{1/2}}{D^*}$$

---

[6] Ibid.

where A = the detector area and is 4×10^{-2} cm^2 for a standard detector

Δf = the bandpass of the detector electronics system and will be assumed to be 5 Hz

The calculated NEP is 1.12×10^{-10} watts, which is the minimum rms power change that can be detected by the detector. The percent of normally incident power at the detector that can be absorbed and recognized as a change is:

$$\frac{1.12 \times 10^{-10} \text{ watts}}{1.59 \times 10^{-5} \text{ watts}} \times 100 = 7.044 \times 10^{-4} \%$$

As previously stated, a 0.01 atm-cm concentration change of CO_2 will provide an absorption change of 2.73 percent. If a 10-cm path-length cell is used, this concentration change is equivalent to a partial pressure change of 0.001 atmosphere. The rate of absorption change is then 2730 percent per atmosphere. The minimum detectable partial pressure change is

$$\frac{7.044 \times 10^{-4}\%}{2.37 \times 10^{3}\%/\text{atm}} = 2.566 \times 10^{-7} \text{ atm}$$

The equation of state for an ideal gas may be evaluated to determine the minimum detectable number of gram moles of gas. The equation is:

$$PV = n\bar{R}T$$

where P = the partial pressure of the CO_2, and in this case is the partial pressure change of 2.566×10^{-7} atm

V = the cell volume, which is 0.004 liters

n = the number of gram moles change causing the partial pressure change

$\overline{R}$ = the universal gas constant 0.08206 atm-liters/gram mole-°K

T = the absolute temperature, and in this case is 283°K

The gram mole change is:

$$n = \frac{PV}{\overline{R}T} = \frac{(2.566 \times 10^{-7} \text{ atm})(0.004 \text{ liters})}{(0.08206 \text{ atm-liters/gram mole-°K})(283°K)}$$

$$n = 4.418 \times 10^{-11} \text{ gram moles}$$

This detectable change is for the detector only and could be decreased by an order of magnitude by the detector electronics and the data processing electronics. Additional reduction in the system detection can be expected when the CO_2 dissolves in the water medium and is not present in the gas cell. However, the reduction is minimal and is discussed in paragraph 3.2, below.

3.2 CO_2 SOLUBILITY IN WATER

The question of evolved CO_2 dissolving in water and not being detected in the infrared cell can be answered by calculations

based on Henry's Law. To calculate the split between gas and liquid phases for CO_2 in equilibrium with water, an ideal solution will be used. This is reasonable, since the solution is diluted and the gas-phase pressure is very low. Using 10°C as the temperature, handbook values show CO_2 solubility to be:

$$m_{CO_2} = 0.2318 \text{ gm } CO_2/100 \text{ gm } H_2O$$

At a CO_2 partial pressure of 760mm, the mole fraction is

$$X_{CO_2} = \frac{0.2318/44}{0.2318/44 + 100/18} = \frac{0.00527}{5.56082} = 9.48 \times 10^{-4}$$

To extrapolate this data to a lower pressure, the Henry's Law constant, K_H, can be used. This is defined as

$$K_H = \frac{P_i}{X_i}$$

where P_i = the partial pressure

X_i = mole fraction

of the i^{th} component. In this case

$$K_{H(CO_2)} = \frac{760}{9.48 \times 10^{-4}} = 8.02 \times 10^5 \text{ mm Hg or } 1.07 \times 10^6 \text{ mb}$$

Now, to calculate the split of CO_2 between the two phases, a situation close to the geometry and conditions of a Mars experiment is assumed. (See Fig. 3-3.)

Geometry = 5 cc gas
2 cc H_2O

Initial = 6 mb CO_2 in gas
at 10°C and equilibrium

Final = 7 mb CO_2 in gas
at 10°C and equilibrium

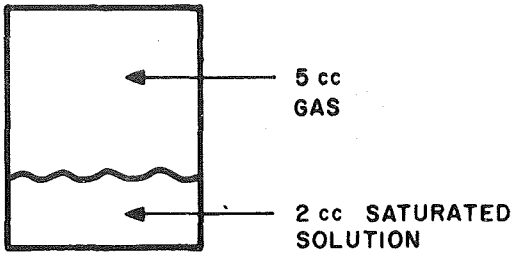

Fig. 3-3 Assumed Geometry and Conditions for Sample Cell

From the Henry's Law constant, the liquid fraction of CO_2 is

$$X_{CO_2} = \frac{6 \text{ mb}}{1.07 \times 10^6} = 5.61 \times 10^{-6} \text{ at 6 mb}$$

$$X_{CO_2} = 6.54 \times 10^{-6} \text{ at 7 mb}$$

Changing this to standard cc, we have

2cc H_2O, or 0.111 moles of H_2O.

Since there are 2.2414×10^4 std cc per mole, then at 6 mb, the gas volume equivalent of dissolved CO_2 is

$$V^{\ell}_{eq_{CO_2}} = X_{CO_2} (0.111)(2.2414 \times 10^4)$$

or

$$V_{eq_{CO_2}}^{\ell} = 1.398 \times 10^{-2} \text{ std cc at 6 mb}$$

$$V_{eq_{CO_2}}^{\ell} = 1.628 \times 10^{-2} \text{ std cc at 7 mb}$$

and

$$\Delta V_{eq_{CO_2}}^{\ell} = 2.30 \times 10^{-3} \text{ std cc from 6→7 mb}$$

For the gas phase, the change is an increase of 1 mb partial pressure. This corresponds to

$$\Delta V_{CO_2}^{g} = \frac{1}{1013} \times 5\text{cc} = 4.92 \times 10^{-3} \text{ cc at } 10°\text{C}$$

Correcting for temperature

$$\Delta V_{CO_2}^{g} = 4.92 \times 10^{-3} \times \frac{273}{283} = 4.75 \times 10^{-3} \text{ std cc}$$

The total gas required to go from 6 to 7 mb at equilibrium is

$$\Delta V_{Total} = \Delta V_{eq_{CO_2}}^{\ell} + \Delta V_{CO_2}^{g}$$

$$= 2.30 \times 10^{-3} + 4.75 \times 10^{-3}$$

$$= 7.05 \times 10^{-3} \text{ std cc}$$

Thus, the percentages are

$$\text{Gas} = \frac{4.75}{7.05} \times 100 = 67.4 \text{ percent}$$

$$\text{Liquid} = \frac{2.30}{7.05} \times 100 = 32.6 \text{ percent}$$

or approximately two-thirds of the CO_2 goes into the gas phase at equilibrium. This relationship holds at any low pressure since ideal solutions show the linear solubility-versus-pressure relationship (Henry's Law).

Therefore, an IR sensor above the liquid would see two-thirds of the CO_2 generated, and its sensitivity would be degraded by only one-third. This argument assumes equilibrium and a pH of 7.0. Obviously, an alkaline solution will have more effect, since CO_2 is more soluble as the solution becomes more alkaline.

In reality, the situation will be even better for actual sensitivity than that shown. If we can again use water at a pH of 7, a real situation will be more like that shown in Fig. 3-4 below.

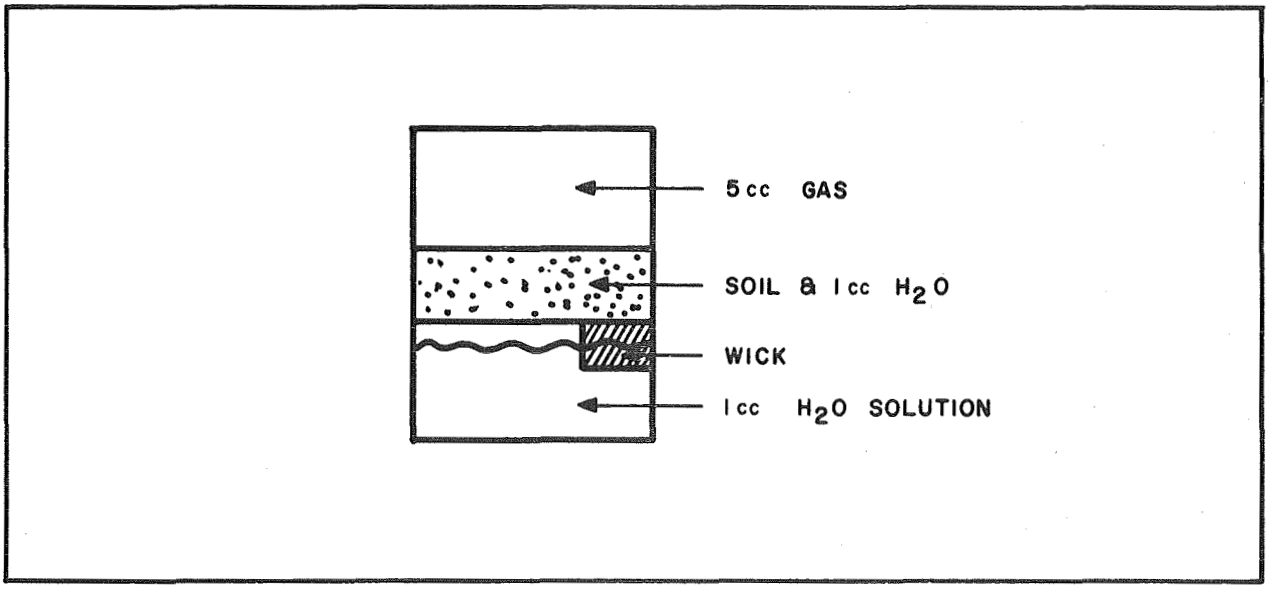

Fig. 3-4 Suggested Sample Cell Configuration

In this case, only half of the water is in contact with the soil, and presumably, most of the organisms producing CO_2 will be in the soil. Thus we can assume that only half of the water comes in direct contact with the CO_2 generated, and the other half will be saturated with CO_2 by a diffusion process. If this is the case (and it is actually closer to reality than the situation previously cited), the amount of CO_2 going to the liquid phase will be approximately one-half of the previous calculation. This is true since the gas above and the liquid below the soil/water sample will receive the CO_2 by a diffusion process. Representative diffusion coefficients for gas and liquid diffusion[7] show that a diffusion process in gas is four orders of magnitude faster than diffusion in liquids. As a consequence, as the CO_2 evolves, the gas phase above will see the change rapidly, whereas the liquid below the soil will lag behind such that its change will be effectively zero in a short time.

Thus, for a real system, the IR sensitivity will degrade by less than 20 percent for measuring changes in CO_2 concentration in the gas above a culture, assuming a pH of 7.

---

[7] R. B. Bird, W. E. Stewart, and E. N. Lightfoot, Transport Phenomena, New York, John Wiley & Sons, Inc., 1960, pp. 495-516.

Section 4
ELECTRONICS

4.1 DETECTOR ELECTRONICS

The electronics used to test the early scatter cells were the same as those developed for the original Wolftrap[1]. These electronics converted the detector current (I_d) into a proportional voltage by using an operational amplifier in a trans-resistance mode. The detector current, generated by a light sensitive diode detector, was proportional to the turbidity of the test solution in the scatter cell. A schematic representation for the electronics is shown in Fig. 4-1.

In every scatter cell tested there existed some ambient light level independent of the solution's characteristics. The ambient light impinging upon the detector resulted from imperfections in the optical focusing of the scatter cell. Not all the light entering the scatter cell left it at a central focus point, but rather some of the light became scattered onto the scatter detector in the absence of any scattering particles. This light caused a diode current to be generated that is referred to as background (I_{bg}). The background light was several orders of magnitude larger than the expected turbidity information. A summing resistor was added to the original electronics to zero out the background current in the trans-resistance circuit, as shown schematically in Fig. 4-2.

---

[1] BBRC, Final Report Engineering Breadboard Model, Wolftrap Microbe Detection Device, F65-6, Sept 8, 1965, pp. 6-3 ff.

This method was used for early tests; however, it was quickly determined that the value of E_1 had to be changed at the beginning of each test run. Since the temperature of the system and the flux output of the light source were held constant, this meant that the optical properties of the scatter cell were dependent upon the fluid introduced into it. Subsequent test verified this and showed a wide dynamic range with the change of background lighting. These tests further proved that the optical properties are often time-dependent (the gaseous content of the solution was generally blamed for the time dependency). The best method for running tests under these conditions was found to be:

1) Induce a sterile fluid media into the scatter cell and allow several hours settling time.

2) Balance out the background with E_1 after the settling time.

Performing the tests in this manner yielded test results of 10^3 to 10^4 organisms per milliliter when testing with E. Coli.

A second problem was experienced during temperature cycling. Large changes in detector output occurred over a temperature change of 20°C. The changes were proportional to the electronic gain. Since the goal of the present design was to increase sensitivity, the temperature dependence was not acceptable. Temperature compensation was achieved by controlling the light flux to the scatter cell, as shown in Fig. 4-3.

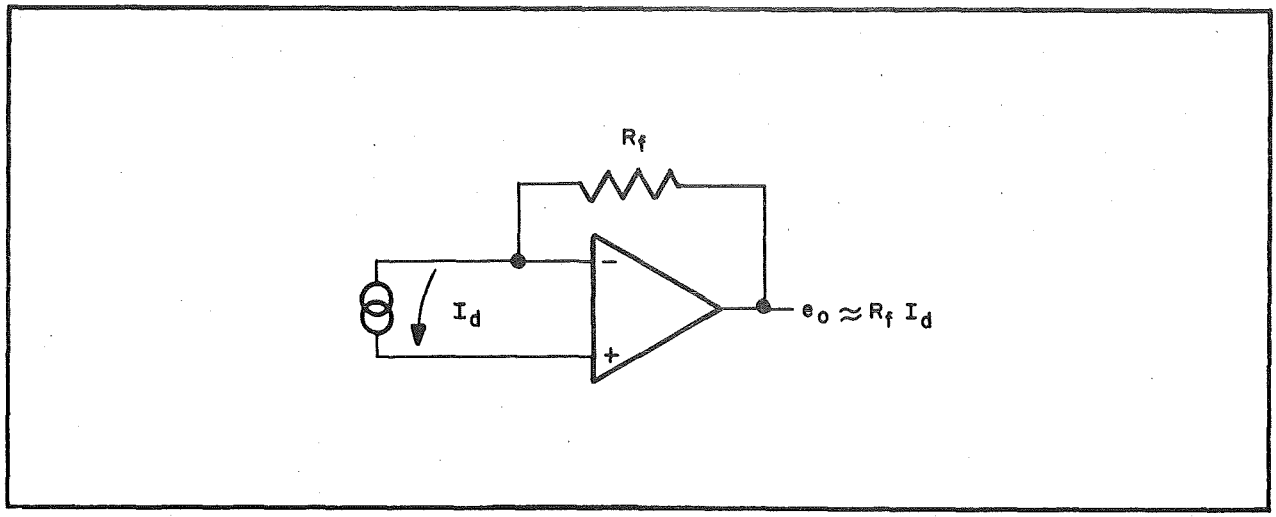

Fig. 4-1 Schematic for Scatter Cell Electronics

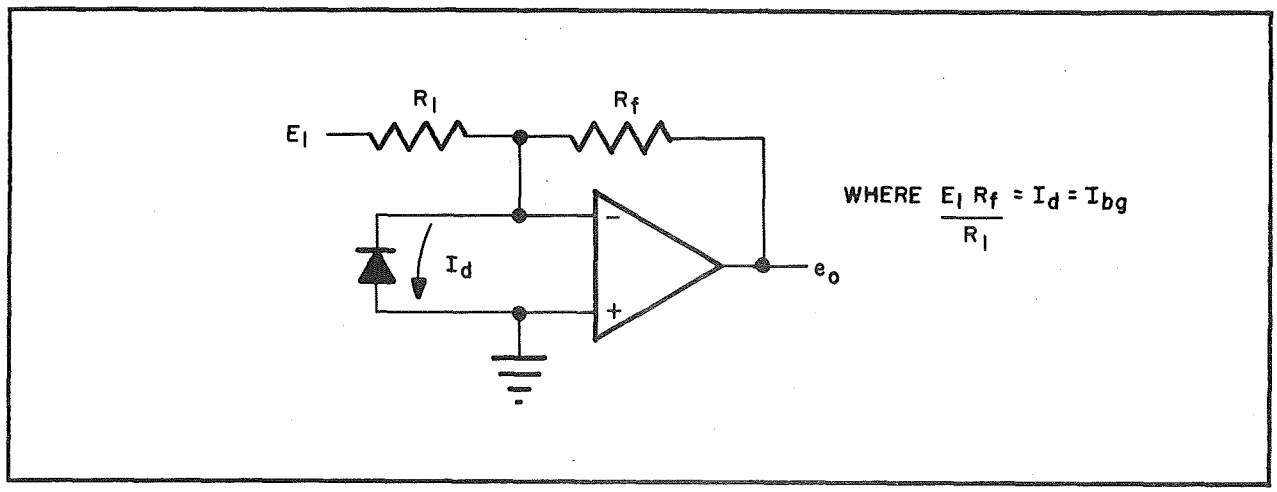

Fig. 4-2 Background-Compensated Scatter Cell Electronics

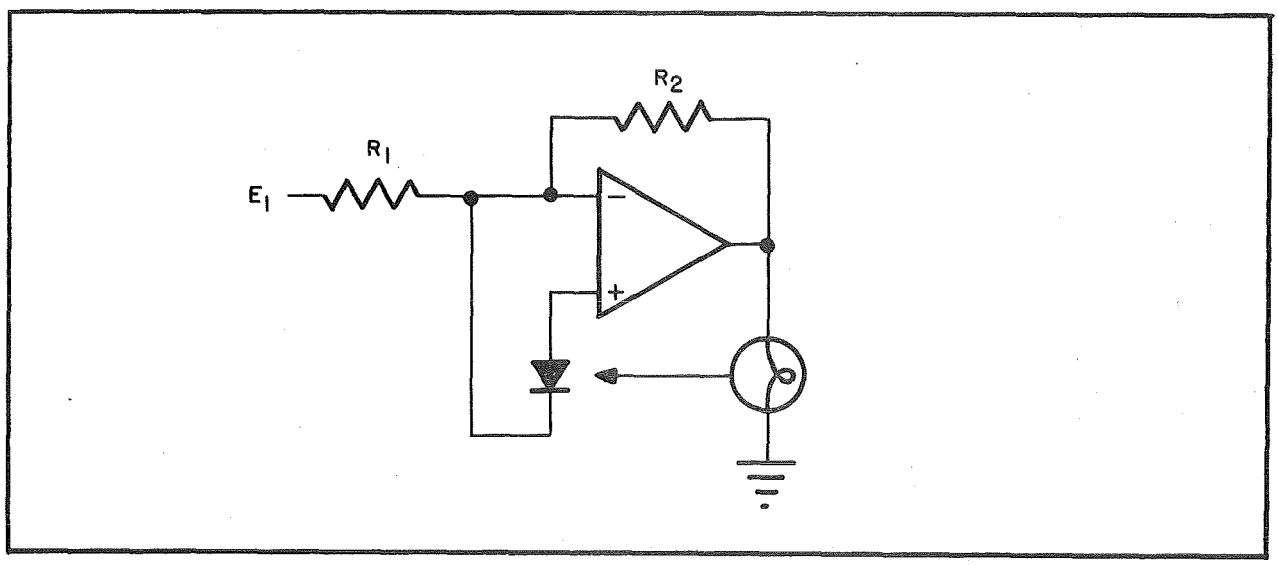

Fig. 4-3 Temperature-Compensated Scatter Cell Electronics

The illuminating source for the scatter cell is a tungsten filament lamp. Its spectral content and intensity are functions of the absolute temperature of the filament. In the past, the lamp power input was used to compensate for detector current errors due to temperature variations. A closed-loop circuit similar to Fig. 4-3 was used to control the source.

R_1, R_2 and E were selected so that the lamp normally conducted approximately 100 milliamperes. Since the lamp irradiated both the control detector and the scatter, and both detectors were held at the same temperature, it was felt that both would receive constant illumination independent of the environment temperature. As the environment temperature increased, larger currents for the same light flux in the control detector would decrease the wattage available to the lamp. This altered the spectral content as well as the source intensity. This resulting change is not bad in itself if the coupling media between the source and the detectors are spectrally identical in both cases. However, past test setups have not accounted for the media difference. The medium from the source to the control detector was air, while that from the source to the turbidity detector was an aqueous solution. Considering the absorption band of water at 0.97 microns (see Fig. 4-4) with respect to the detector and lamp spectral characteristics, it becomes apparent that the correspondence between the two detector illuminations is not 1-to-1. The control of the light source with a secondary detector does not seem to be an optimum approach except in a case where the coupling media are identical. The use of nutrients in the scatter cell solution can further compound the problem.

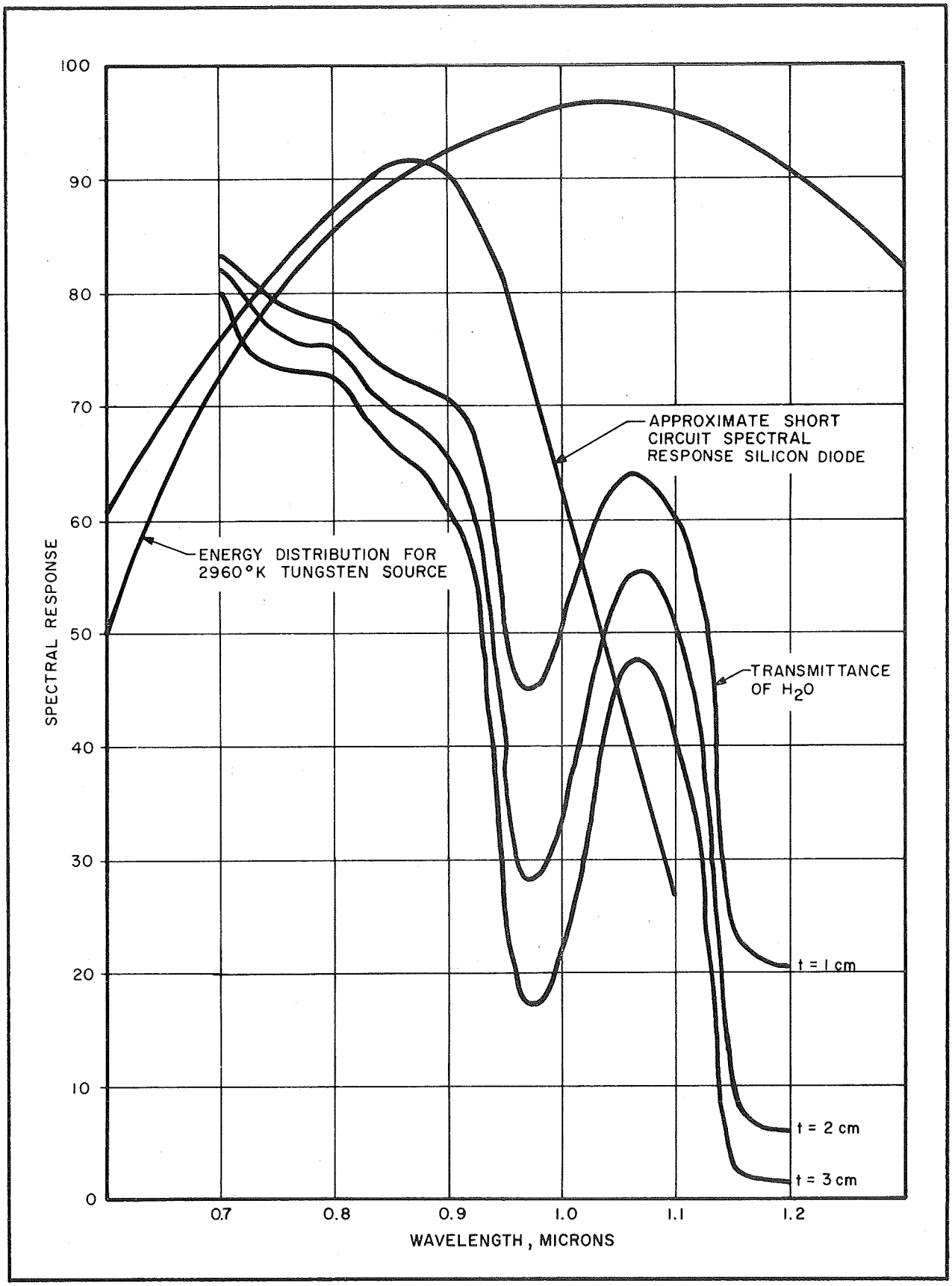

Fig. 4-4 System Spectral Characteristics

Testing of the scatter cells with the previous temperature and background compensation systems proved unsatisfactory. The conclusion reached from the test analysis was that the original design must be modified, especially for the high gains required for the desired increase in sensitivity. In the final analysis, the major problem was that the detector electronics were single-ended. That is, there was no reference signal that was a function of the thermal or optical environment. Thus, an error signal occurring because of a thermal or optical change appeared in the output as turbidity datum.

In recognition of this problem, a true differential scatter cell was tried. This means that a detector should be provided for the reflected nonscattered light. In addition, the path length and media for this detector must be identical to those of the scattered light. Thus, the spectral characteristics of the reflected light would be the same as for the scattered light over the temperature range. In addition, the fluid properties of the media would modify both reflected and scattered light identically. This reflected light then illuminates a second detector, which acts as a reference source for differential measurement. The two light detecting diodes must be held at the same temperature. The scatter cell configuration that was tested is shown in Fig. 2-8.

The electronics used to test the scatter cell are shown in Fig. 4-5.

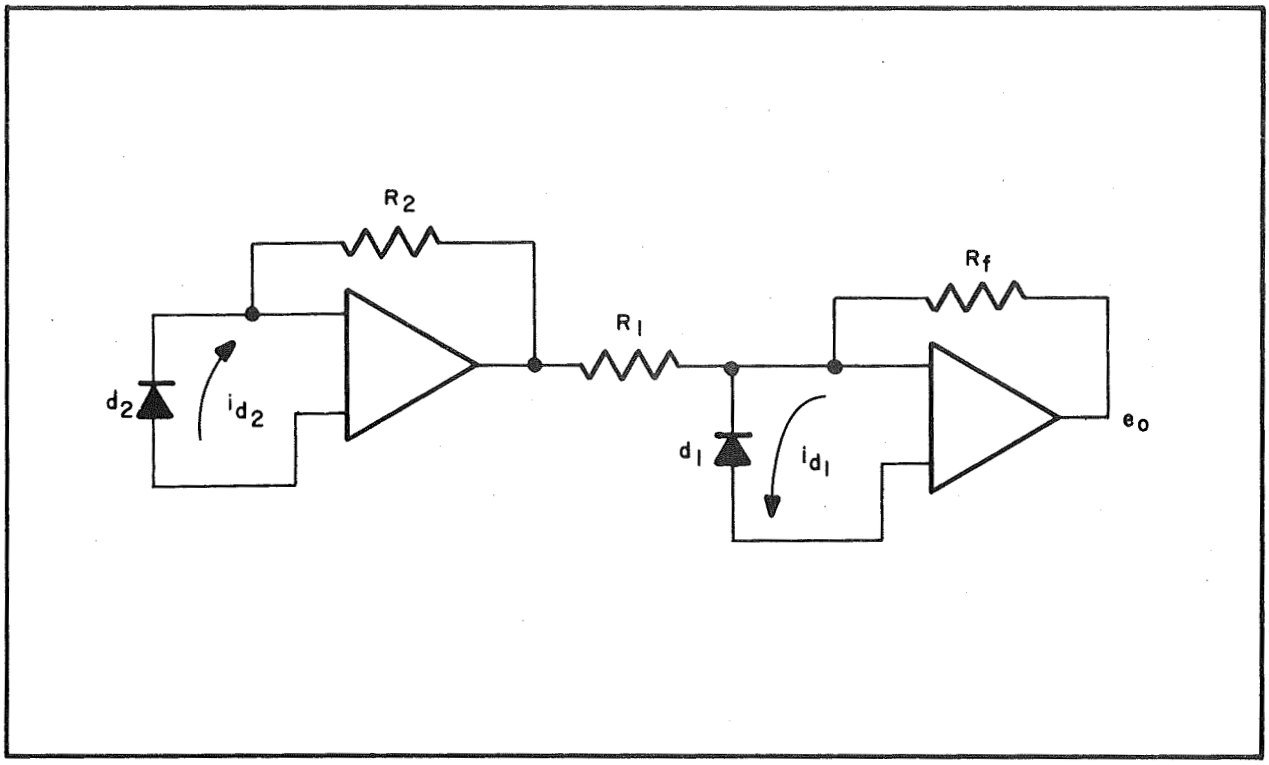

Fig. 4-5 Differential Scatter Cell Electronics

In this circuit, R_1 and R_2 were chosen so that under quiescent conditions e_o would be zero. This allows a differential measurement using d_2 as the reference. The voltage equation for e_o is:

$$e_o = (i_{d_1} - i_{d_2} \frac{R_2}{R_1}) R_f$$

where $i_{d_1} = i_{bg_1} + \Delta_1$

$$i_{d_2} = i_{bg_2} - \Delta_2$$

and Δ_1 and Δ_2 are the incremental currents caused by scatter due to the turbidity of the solution. Substituting for i_{d_1} and i_{d_2}

$$e_o = (i_{bg_1} + \Delta_1 - i_{bg_2} \frac{R_2}{R_1} + \Delta_2 \frac{R_2}{R_1}) R_f$$

If

$$i_{bg_1} = i_{bg_2} \frac{R_2}{R_1}$$

then

$$e_o = (\Delta_1 + \Delta_2 \frac{R_2}{R_1}) R_f$$

Thus, the background currents are made equal and cancel, while the incremental currents sum.

The differential system was put together to attempt a design confirmation. It was felt that a properly balanced differential system should remain so over wide illumination changes. Brief testing on the model appeared encouraging; however, time expired before comprehensive tests could be performed.

In summary, the problems encountered using the original Wolf Trap electronics required an alternate approach. A single-ended system that must process large thermal and optical error sources while accommodating small signals cannot operate successfully. The analysis and limited testing on the differential system looked promising, and must be considered as a strong alternate design approach.

4.2 ELECTRONIC NOISE

In scatter cell testing, a design goal of 10^3 organisms/milliliter was used. To achieve this limit the electronics require 10^8 ohm feedback resistors in the trans-resistance circuit. Detector currents of 1 nanoamp produce a voltage output of 100 millivolts. Test data indicated that 0.5 nanoamp accuracy was required to

successfully measure 10^3 organisms/milliliter. Operation in this current range is difficult because of the large noise signal generated, particularly the 1/f noise in the detecting diodes. Noise voltages of 200 millivolts peak-to-peak were experienced, or currents of 2 nanoamperes. Obviously, under these conditions, the desired sensitivity cannot be obtained.

In general, the mean-squared noise current for a junction diode (excluding 1/f noise) is given by:

$$i_d^2 = 2e(I + 2I_o)\Delta f$$

where e = electron charge
I = current flowing through the diode
Δf = bandwidth
I_o = reverse bias leakage current

Since the detector diode has a large surface area, I_o becomes large and is in the neighborhood of 5 μamps. Thus

$$i_d^2 = 2 \times 1.6 \times 10^{-19} \times 2 \times 5 \times 10^{-6} \Delta f$$

$$= 32 \times 10^{-25} \Delta f$$

$$= 3.2 \times 10^{-24} \Delta f$$

$$i_d = 1.79 \times 10^{-12} \sqrt{\Delta f}$$

Therefore

$$e_o = 1.79 \times 10^{-4} \sqrt{\Delta f}$$

For the required sensitivity, e_o must be less than 1.0 millivolt due to noise. Then

$$\sqrt{\Delta f} = 5.57$$

$$\Delta f = 25 \text{ cycles}$$

Therefore, for the required sensitivity, the detector electronics should be operated well above the 1/f region and have a bandwidth of less than 25 cycles. This analysis does not consider the referred input noise of the operational amplifier. However, the amplifier should be operated above 1 Hz to limit its 1/f noise. Since the amplifier is used in a trans-resistance mode, only the referred input voltage should appear at the output and this can be kept low at the higher frequencies.

The requirement for ac or chopped operation requires that the source be also capable of this type operation. This requires either

1) A mechanical chopper for a tungsten source.

2) A light-emitting source with sufficient frequency response to accommodate the system, i.e., a light-emitting diode.

Operation on ac also requires that the detector have the required frequency response. This generally means that the diode must operate in the short circuit mode and be loaded with very little capacity.

In summary, the achieve the required sensitivity, dc operation is not adequate. The turbidity signal must be chopped and demodulated to meet a design goal of 10^2 to 10^3 organisms per milliliter.

4.3 DATA HANDLING

According to ASO RFP A-14859AG-1, B-7 the "anticipated data transmission available for life detection instrument is 10^4 bits." The 10^4 bits were interpreted to be the total for a 30-day mission. This 10^4 bits must accommodate not only detector data, but also control and housekeeping. The following assumptions were made in establishing the data handling system.

1) No more than eight scatter detectors to monitor in a given 30-day period.

2) Each scatter cell measurement will be made in conjunction with another independent life detection system, i.e., IR absorption, pH, or conductivity.

3) Critical housekeeping functions shall be monitored and compared against an on-board standard and transmitted:

   - Only if a no-go situation exists during a measurement period,
   - Every 4 to 24 hr period of operation.

4) Non-critical housekeeping functions shall be transmitted every 4 to 24 hour period of operation.

5) To accommodate for the large dynamic range of the scatter output, some form of data compression will be used.

Since no information is available concerning expected growth rates on Mars, it is difficult to pick a fixed time sampling system that would be optimum. A system that would only transmit significant changes would best satisfy the limited data rate. However, this system does require on-board memory so that previous measurements can be compared with new ones. The size of the on-board memory would be a function of the bits required to adequately describe each measurement. Assuming a dynamic range of $<10^5$, the word length required to report back each one-quanta change in data, using the natural log — arithmic base as a worst case, would be 8 bits, consisting of 4 bits for the characteristic and 4 bits for the mantissa. Thus, for sixteen measurement points the memory would require 128 bits to store a complete data sample. This size memory is easily implemented using MOS FET shift registers.

The data handling system proposed then is as follows:

1) Detector Outputs — The detector outputs will be 0-10 volt signals with 3 decades of resolution. Additional discrete data bits will represent gain settings.

2) Analog to Binary Conversion — Each detector analog output will be converted to a 10-bit binary word. This will yield ±10 millivolts resolution for the analog data.

3) $\ln_e$ Generator — The detector binary data and discrete data will be operated upon to generate an 8-bit $\ln_e$ representation of the data.

4) $\ln_e$ Sampling – The $\ln_e$ data will be stored and compared for changes at each measurement point. A change of two or more in the binary equivalent of the mantissa will cause a sample point to be transmitted.

5) Scatter Cell Sampling – The scatter cell shall be sampled at fixed time intervals. The sample period shall be commandable. The maximum rate will be consistent with the power budget available.

6) Housekeeping Data – This data shall not exceed 2048 bits total for a 30-day period. Thus for each 24-hr period, eight 8-bit words will be acquired.

The block diagram for the data system is shown in Fig. 4-6.

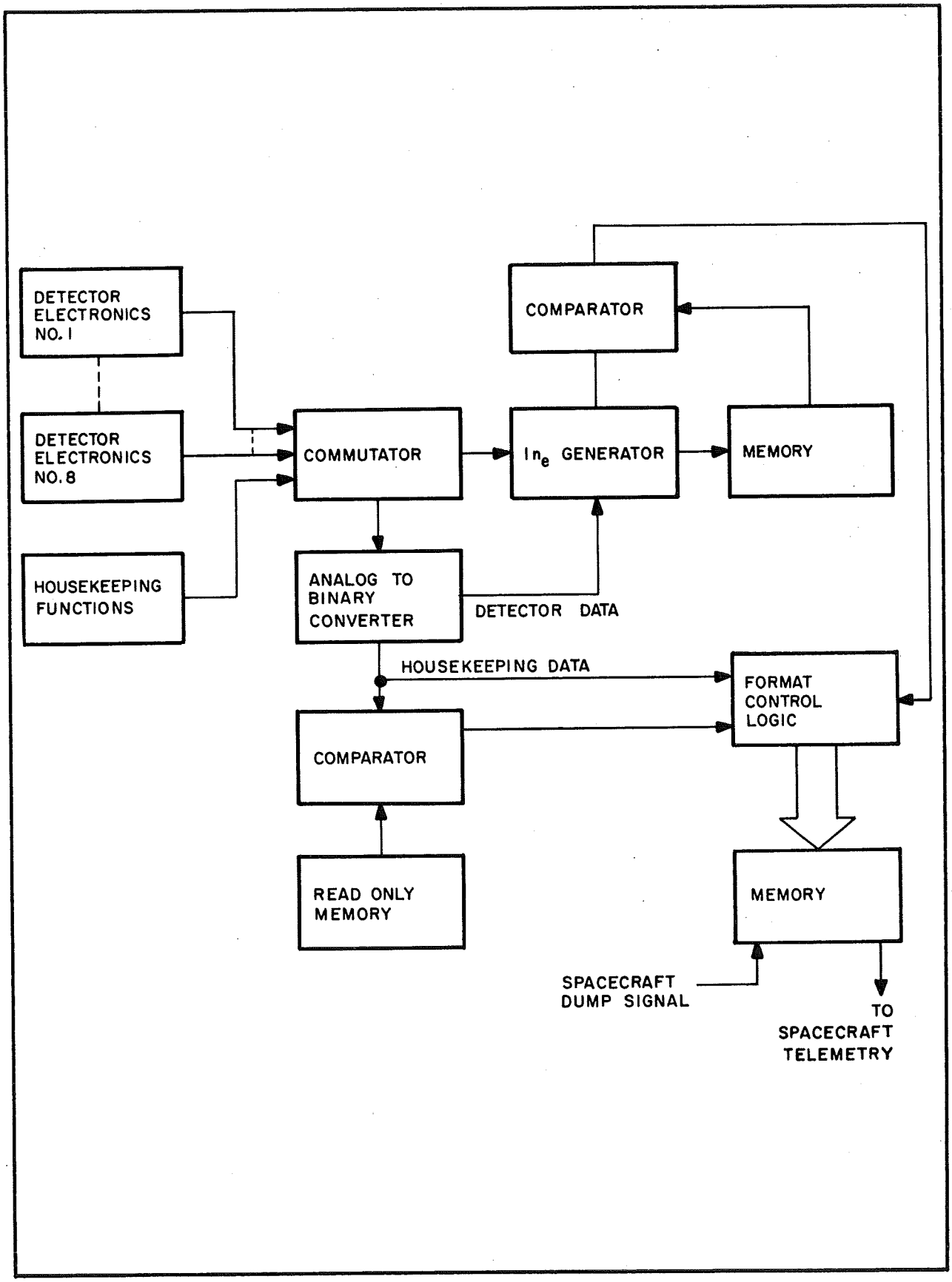

Fig. 4-6 Data System Block Diagram

Section 5
SYSTEM DESCRIPTION

Once the general scientific objectives and techniques were defined, the engineering design effort was begun with the aim of translating these objectives into a mechanical system capable of performing all the necessary tasks. These tasks were grouped into four major categories, each of which could be separately modeled and tested to prove feasibility:

1) Soil handling and sample distribution

2) Liquid handling and soil extract preparation

3) Light scatter cell

4) IR absorption cell

It became apparent very early that the scientific objective of conducting the experiments over a span of ninety days, together with the constraints of weights, comprised the major problem area in developing an instrument design that would meet all the requirements. Although the purpose of this study was to recommend a design for a science breadboard, it seemed prudent to consider the design, within time limits, in terms of a flight-configured system.

5.1 SUBSYSTEM DEFINITION

The initial effort was directed toward breaking the four major categories down into elementary functions. With such a "task

list" we could then examine the individual functions, and their relationships to each other, and attempt to reduce the overall complexity of the system by having certain elements relate to more than one function. The minimum "task list", grouped for each of the four categories, follows.

Soil Handling Subsystem

1) Provide a soil hopper common to all sample chambers. The hopper must receive the soil sample provided from the lander vehicle, be mechanically capable of moving it to the individual assay chambers when commanded, and signal that it has reached there.

2) The hopper should be able to verify the receipt of bulk soil from the lander and detect the amount of soil received. It should generate a signal to the soil supply system to indicate when it is filled.

3) The hopper must move on command to any assay chamber station, from a random position, and signal when it reaches there.

4) A soil dispensing device should be incorporated as a part of the hopper. The dispenser should be capable of dispensing measured amounts of soil from the hopper to be used as assay samples. Each allotment should be separated into two samples, one to be used to prepare a soil extract, the other

to be used as the inoculum. The two samples need not be equal in volume, but the ratio between them would remain fixed. The sample amounts may be made to vary from cell to cell.

5) The depletion of soil from the hopper should be detected and accepted as verification of actual disbursement.

6) The soil hopper must have a "dump" station where the excess soil, left in the hopper after all the sample chambers have been filled, may be dumped.

7) The sample chambers must be open to receive samples from the dispenser, and be capable of sealing from the atmosphere, on command, before the assay period. One or all soil chambers may be filled as the initial operation, with the assay period for each chamber to be subsequently initiated as desired.

8) The assay cell should be filled with Mars gas, at ambient pressure, before sealing it to commence an assay. The gas should not contain any contaminants from the retro-rockets.

9) After sealing, the cell must be over-pressured to a level sufficient to inhibit vaporization of the water in the soil extract.

Soil Extract Preparation

10) Rupture a liquid storage vessel and provide a path from the vessel to the primary soil sample. Introduce sufficient fluid pressure to diffuse the liquid through the sample and filter. Collect the filtered extract in the light scatter cell.

11) Maintain an accurate control of the extract volume to prevent overfilling the light scatter cell.

Light Scatter Cell

12) The light scatter cell is primarily an optical detection system, as discussed in Section 2. Its mechanical requirements are that it have the required fluid capacity and be insensitive to an attitude up to 34 degrees from vertical. It must also be designed to allow the extract to capillary up to the "dry" soil sample, from which inoculation can take place by either migration or mass transfer through the capillary bridge.

IR Absorption Cell

13) Provide an enclosed cell having a connecting passage to the soil sample. This forms a part of the assay chamber when sealed off from the ambient atmosphere. The partial pressure of CO_2 within

this portion of the chamber is then measured and monitored for changes, as described in Section 4.

14) The IR optical system must be common to all cells. It consists of an energy source, a reference cell identical to the sample cells, a light chopper, conditioning optics, and a detector.

15) The entire IR optical system must be indexed, on command, to any sample cell and make IR absorption measurements in that cell. A signal must be generated to indicate when the system reaches the commanded station.

5.2 PROBLEM AREAS

Having identified the elements and functions of which the instrument would likely consist, we then identified problem areas. The most important of these are:

1) Highly reliable energy sources

2) Seals and valves

3) Liquid storage

4) Effects of dry heat sterilization

5) Particulate filtering of the soil extract

Energy Sources

Electric motors, solenoids, springs, and compressed gas were considered as energy sources.

Compressed gas was discounted for the following reasons:

1) It would have a weight disadvantage because of the many valves and actuators that would be necessary.

2) After rupturing the seal for initial use on Mars, a highly dependable system of valves and seals would be required to preserve the pressure for the 90-day mission life. This could be a problem, particularly if helium were used as a power gas, because of the permeability of most seal materials.

Solenoids did not appear to be desirable because, due to their short stroke relative to size and weight, their motions often have to be amplified by levers. This affects any weight advantage and the resulting mechanical disadvantage may render them marginally reliable.

Electric motors were selected as a good candidate as an energy source for several reasons:

1) They are small in size.

2) They are lightweight.

3) They can move in two directions.

4) Their torque is easily multiplied with light-weight gears.

5) BBRC has a great deal of experience in lubrication of motors for space use, so that this may substantially be ruled out as a problem.

6) Both synchronous and stepper motors may be applicable, and each is being evaluated.

Within the scope of their capability, springs are a very good candidate as a source of power because:

1) Their energy can be stored almost indefinitely.

2) Energy release is simple and reliable.

3) With correct selection of materials, they are almost entirely unaffected by a hostile environment.

Seals and Valves

Seals and valves have been considered as a necessary evil, to be avoided if possible. Consequently, the presently recommended design has no valves, and no dynamic seals. Valves have been eliminated through the use of discrete liquid storage vessels for each cell, and the only moving part that requires a seal (the sample chamber) uses a static O-ring seal of a valve-seat design.

This design is intended to solve the problems that could be

expected in dynamic seals due to deformation during sterilization. Also, because of possible adhesion between the seal and the metal during space voyage, a dynamic seal could be damaged by the break-away action in operation and made ineffective.

Because the seal in the present design will not be squeezed during heat sterilization, there will be no tendency to deform. It also does not require any breakaway force, thus lending itself to more reliable activation.

Filters

Filtering of the soil and water mixture is necessary to produce a particulate-free extract of soluble nutrients supplied to the light scatter cell. A test program was performed to determine the best readily available filter for repeated feasibility testing. Summary results are as follows:

1) Soil sample - composite of local gold-mine settling-pond residue and mountain sedimentary formation, both containing much claylike material.

2) Filter components - Whatman borosilicate glass-fiber mat filters, graded GFA (coarse) and GFC (ultra-fine), and autoclavable cellulose triacetate membrane filter discs.

3) Filter combination - the best combination of filters for maximum particulate extraction in the minimum time, is a 2mm-thick stack consisting of:

   a. GFA (top side nearest sample)

b. GFA
c. GFC
d. 5-micron pore membrane
e. GFA (separator)
f. 1.2-micron pore membrane
g. GFA (separator)
h. 0.45-micron pore membrane
i. 0.22-micron pore membrane

In general, two coarse prefilters are necessary on top to prevent the membrane filters from plugging. Addition of a third coarse filter doubles the required filter time. Coarse separators, which could be fine mesh screen, are necessary between the larger-pore membrane filters. Active filter area is 10.75 square centimeters.

4) Sample preparation - 102 grams of composite sample in 170 ml distilled water, with no detectable difference in performance whether boiled or cold mixed.

5) Pressure differential - 5 psig from vacuum pump.

6) Filter rate - 1.1 ml/min/cm^2 filter area, average for required total time 15-minutes.

7) Water recovery - 34 milliliters water hangup, mostly in sample residue.

8) Filtrate - light straw color with no visual evidence of colloids.

5.3 SYSTEM CONFIGURATION

A system configuration having the sample cells in line was an early consideration. This arrangement had some disadvantages, however, in the support structure for the moving soil hopper, and in the linear bearings. The bearings have some problems of lubrication, and require special attention, such as boots, to keep the shafts clean.

The system configuration that appears most desirable is the rotary or carousel type, with the sample cells arrayed in a circle.

A turntable is mounted on an 8.0-inch inside-diameter ball bearing, having a rated capacity of 3500 lbs radial load, and 8800 lbs thrust load. The bearing weighs only 0.38 lb. The turntable is rotated by a stepper motor in contact (through a 40-to-1 worm gear reduction) with gear teeth at the rim of the turntable. The resulting resolution per motor step is about 1.5 arc-minutes. Supporting the rotating table at its outer diameter gives a structurally rigid member upon which to mount the elements that traverse between sample cells, thus avoiding a cantilevered arrangement of rotating members supported from a central bearing. Also, the platform design is not hampered by the unusable space that would otherwise be occupied by a central support.

The elements that mount to the turntable are:

1) The soil hopper

2) The soil dispenser

3) The IR optical system

Figure 5-1 is a sectional view of an early concept, which has an array of 15 experiments. The IR system is also shown conceptually and comprises a tuning fork chopper with a dual-wavelength filter. Alternate passing of a wavelength corresponding to the absorption band of CO_2 and a reference wavelength provides a measure of CO_2 within the chamber. Further analysis of this IR detector indicated that it lacked the desired level of sensitivity and a separate study was conducted. This is presented in Section 4.

Using 10 lbs as a weight budget, it was decided to determine the maximum number of experiments that could reasonably be included in this carousel system. Preliminary analysis indicated that 18 was an attainable number, and another layout (Fig. 5-2) was made based on this objective. However, this proved to be overly ambitious because of the refinements to the IR system, which will weigh considerably more than it did in the oversimplified first-cut.

Using the concepts included in the systems of Figs. 5-1 and 5-2, a sample-processing feasibility model was designed. The layout is shown in Fig. 5-3. This model includes functional components which can be easily separated for testing. The bridging tendency of soil was to be overcome by the "knocker" cam located on the measuring drum shaft, which supplies a sharp rap from a spring-loaded hammer every 90 degrees of rotation. The IR detector was not included, because separate feasibility tests were to be performed on another model. Detailed drawings were prepared for the

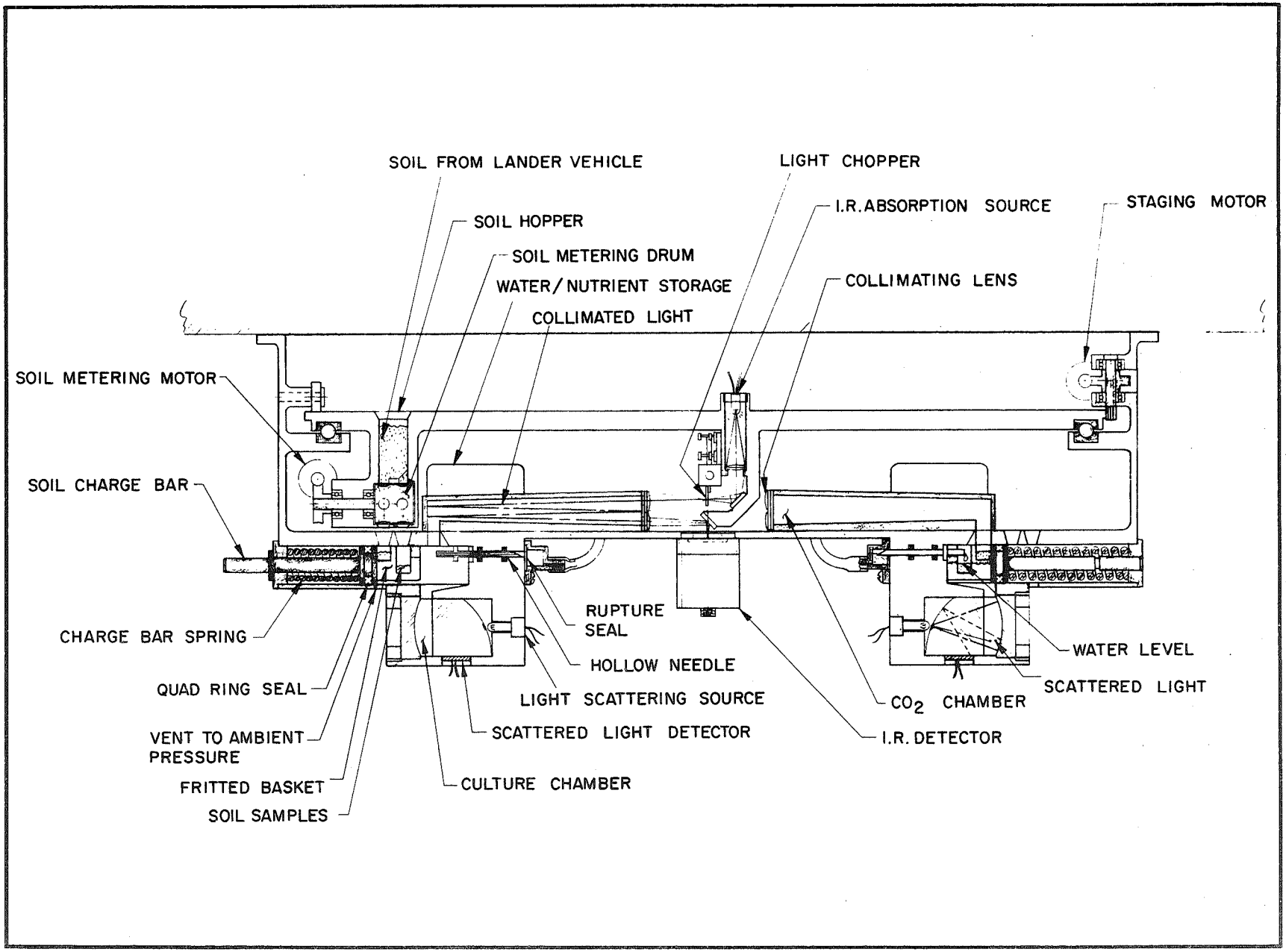

Fig. 5-1 Early System Concept

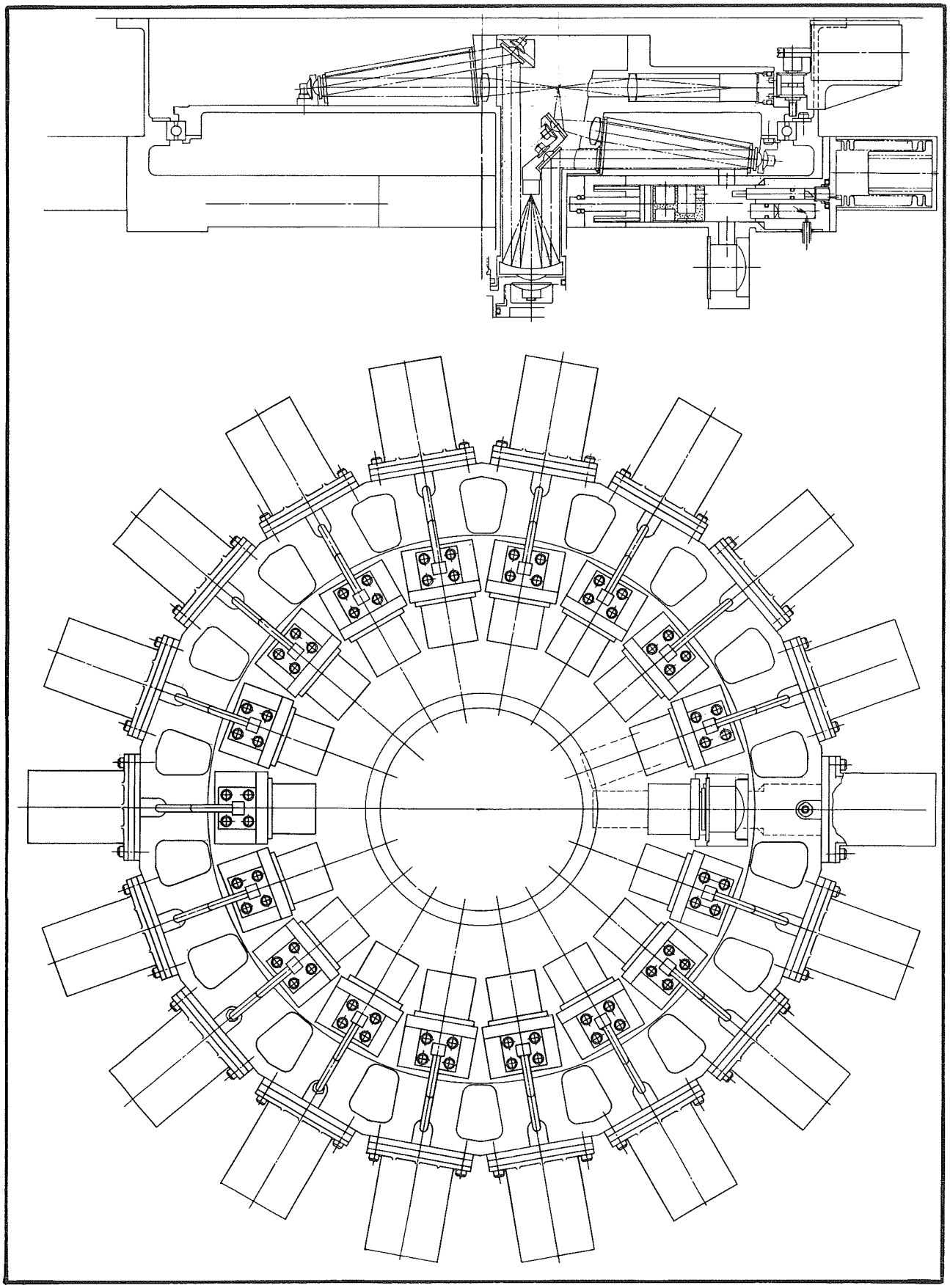

Fig. 5-2 Eighteen-Cell System Concept

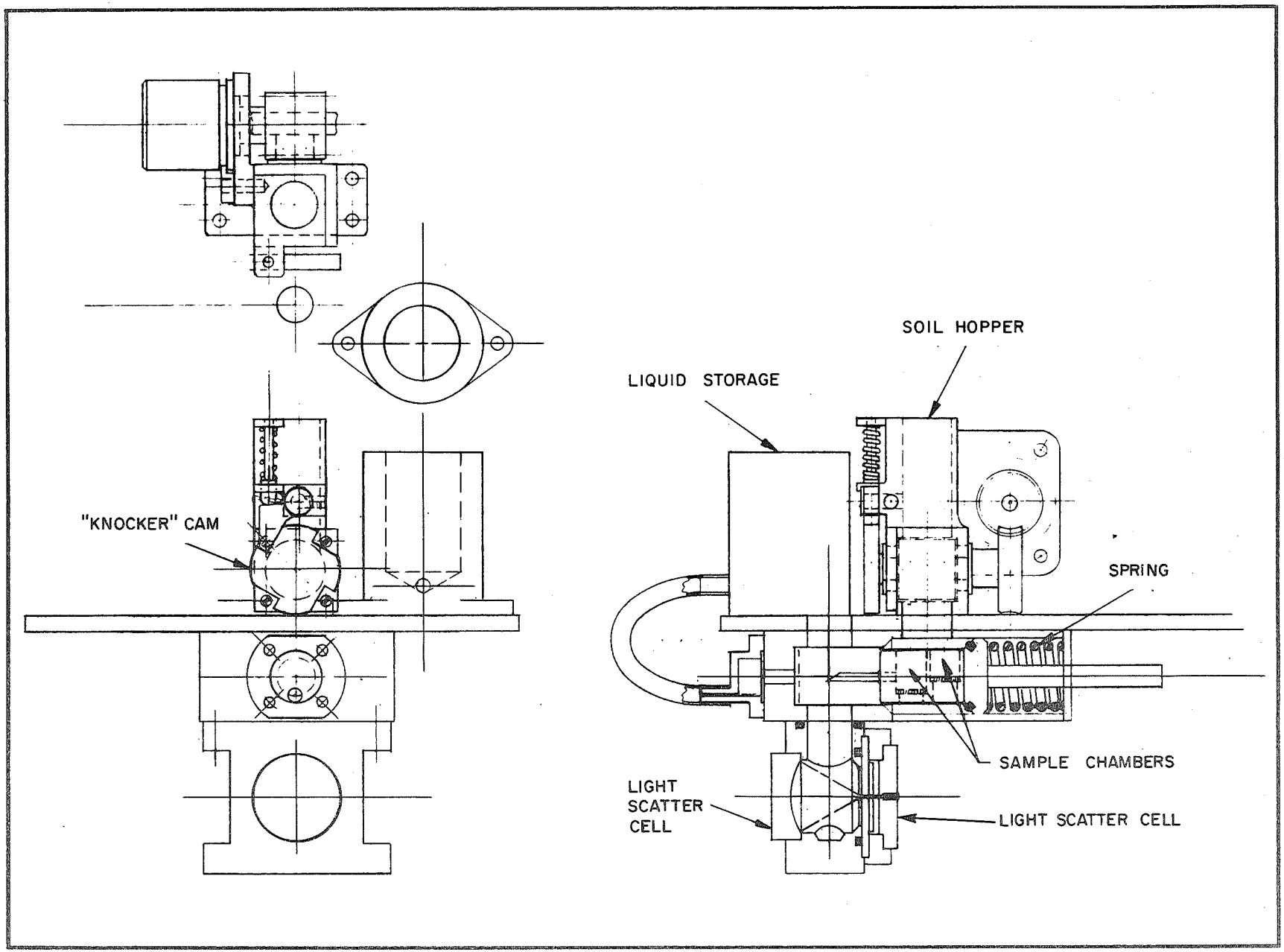

Fig. 5-3 Sample Processing Feasibility Model

sample processing model, but lack of funding has not permitted fabrication.

Subsequent to the completion of the feasibility model design, the IR detector design and the soil-water filtering tests were completed. The number of sample cells decreased to nine because of increased size of the IR detector and required forced water filtering of the soil sample. The latter requirement increased the size of the sample chambers to accommodate the filter stack. The final flight-configured concept is shown in Fig. 5-4. The estimated weight is 10 lbs including electronics.

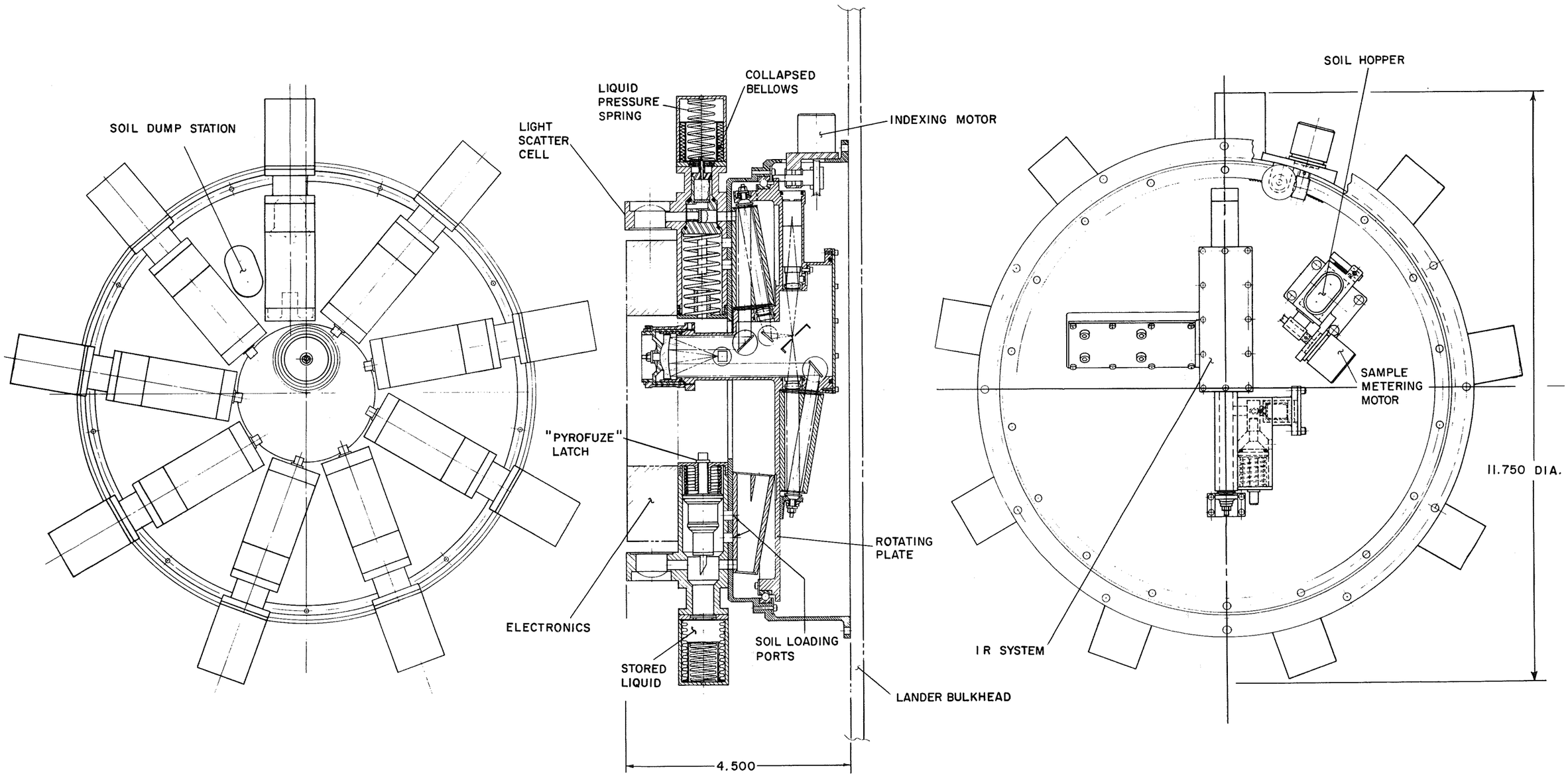

Fig. 5-4 Flight Configuration Concept